Hydrocarbon source signatures in Houston, Texas: Influence of the petrochemical industry

B. T. Jobson,[1] C. M. Berkowitz,[1] W. C. Kuster,[2] P. D. Goldan,[2] E. J. Williams,[2] F. C. Fesenfeld,[2] E. C. Apel,[3] T. Karl,[3] W. A. Lonneman,[4] and D. Riemer[5]

Received 9 April 2004; revised 20 August 2004; accepted 14 October 2004; published 22 December 2004.

[1] Observations of C_1-C_{10} hydrocarbon mixing ratios measured by in situ instrumentation at the La Porte super site during the TexAQS 2000 field experiment are reported. The La Porte data were compared to a roadway vehicle exhaust signature obtained from canister samples collected in the Houston Washburn tunnel during the same summer to better understand the impact of petrochemical emissions of hydrocarbons at the site. It is shown that the abundance of ethene, propene, 1-butene, C_2-C_4 alkanes, hexane, cyclohexane, methylcyclohexane, isopropylbenzene, and styrene at La Porte were systematically affected by petrochemical industry emissions. Coherent power law relationships between frequency distribution widths of hydrocarbon mixing ratios and their local lifetimes clearly identify two major source groups, roadway vehicle emissions and industrial emissions. Distributions of most aromatics and long chain alkanes were consistent with roadway vehicle emissions as the dominant source. Air mass reactivity was generally dominated by C_1-C_3 aldehydes. Propene and ethene sometimes dominated air mass reactivity with HO loss frequencies often greater than 10 s^{-1}. Ozone mixing ratios near 200 ppbv were observed on two separate occasions, and these air masses appear to have been affected by industrial emissions of alkenes from the Houston Ship Channel. The La Porte data provide evidence of the importance of industrial emissions of ethene and propene on air mass reactivity and ozone formation in Houston. *INDEX TERMS:* 0345 Atmospheric Composition and Structure: Pollution—urban and regional (0305); 0365 Atmospheric Composition and Structure: Troposphere—composition and chemistry; 0322 Atmospheric Composition and Structure: Constituent sources and sinks; *KEYWORDS:* hydrocarbons, sources, variability

Citation: Jobson, B. T., C. M. Berkowitz, W. C. Kuster, P. D. Goldan, E. J. Williams, F. C. Fesenfeld, E. C. Apel, T. Karl, W. A. Lonneman, and D. Riemer (2004), Hydrocarbon source signatures in Houston, Texas: Influence of the petrochemical industry, *J. Geophys. Res.*, *109*, D24305, doi:10.1029/2004JD004887.

1. Introduction

[2] The atmospheric oxidation of hydrocarbons (RH) plays a central role in understanding the formation of ozone and particulate matter in the troposphere. Hydrocarbon oxidation is primarily initiated by the hydroxyl radical (HO). These reaction mechanisms are complex but their essential feature is the radical chain carrying reactions between peroxidic radicals and NO that regenerate HO and form NO_2. In the daytime NO_2 rapidly photolyzes to yield ozone. Given high enough peroxy radical and NO concentrations and the right meteorological conditions, ozone can rapidly accumulate on both urban and regional scales [*Solomon et al.*, 2000] to concentrations that are though to be injurious to human health [*Lippmann*, 1991]. Hydrocarbon oxidation products can be of low enough volatility that they will partition onto existing particulate matter, contributing significantly to fine particle mass as secondary organic aerosol [*Schauer et al.*, 2002]. In urban areas the formation of ozone and particulate matter are thus entwined through hydrocarbon chemistry.

[3] Understanding how to control ozone and particulate matter concentrations in urban and rural areas has been an ongoing challenge for many decades. It was first recognized that ozone was photochemically produced from mixtures of hydrocarbons and nitrogen oxides in the early 1950s [*Haagen-Smit*, 1952]. Motor vehicles were recognized as important sources of CO, NO_x and VOCs and vehicular emissions controls were introduced in the United States in the early 1970s. Since then it is estimated that while vehicle miles traveled has more than doubled, the on road vehicle emissions of CO and VOC have been reduced by 43 and 59% respectively while NO_x emissions have remained level [*Environmental Protection Agency* (*EPA*), 2000]. Major sources of anthropogenic hydrocarbons in the United States

[1]Pacific Northwest National Laboratory, Richland, Washington, USA.
[2]NOAA Aeronomy Laboratory, Boulder, Colorado, USA.
[3]Atmospheric Chemistry Division, National Center for Atmospheric Research, Boulder, Colorado, USA.
[4]National Exposure Research Laboratory, Senior Environmental Employment Program, U.S. Environmental Protection Agency, Research Triangle Park, North Carolina, USA.
[5]Rosenstiel School of Marine and Atmospheric Science, University of Miami, Miami, Florida, USA.

Copyright 2004 by the American Geophysical Union.
0148-0227/04/2004JD004887

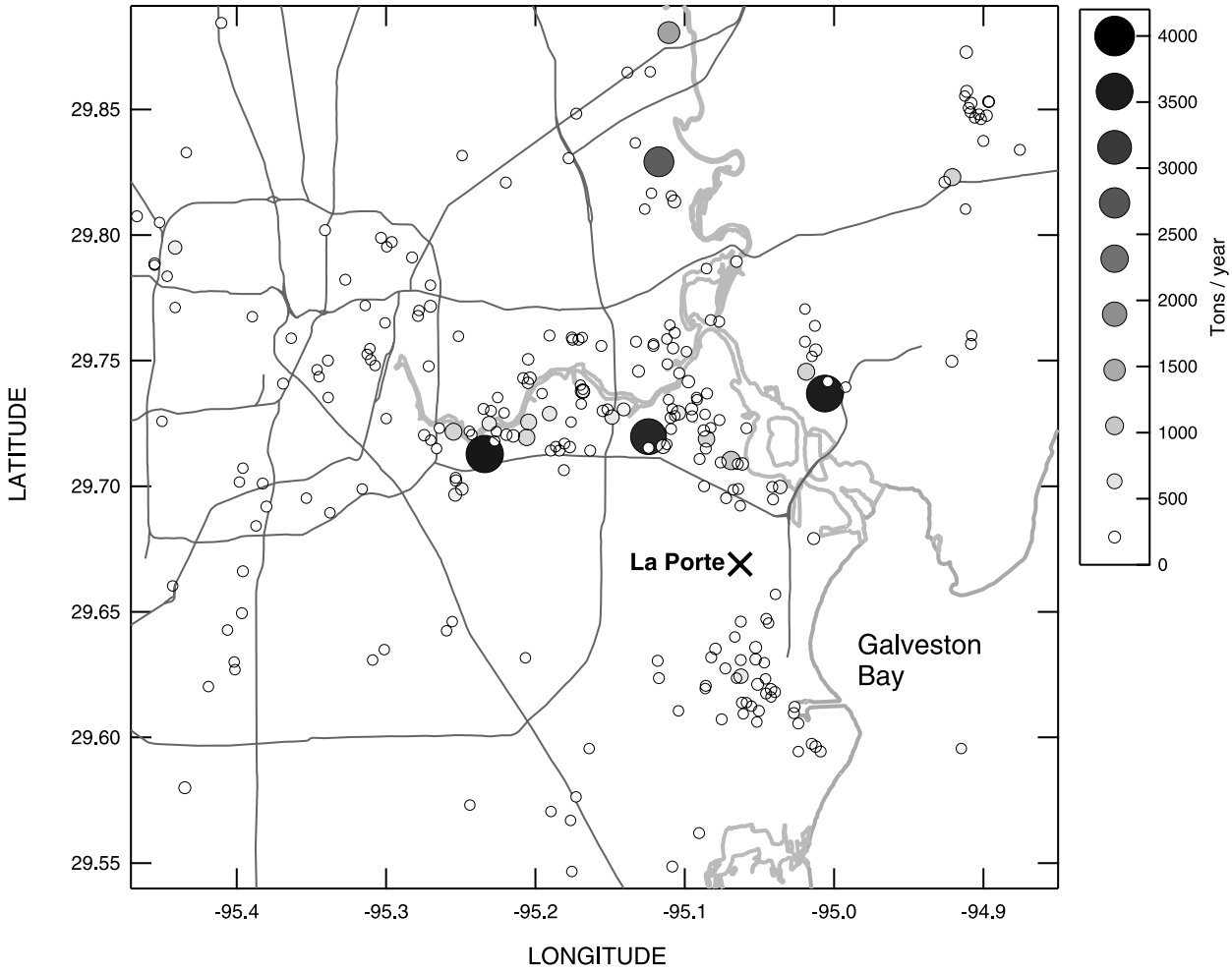

Figure 1. Map of the Houston study region showing the La Porte study site in relation to major highways, the Houston Ship Channel, and major hydrocarbon point sources. Point sources are color- and size-coded according to mass emission rates given by the legend.

include on road vehicle emissions, solvent use, nonroad engines and vehicles, fossil fuel storage and transport, and industrial emissions [*EPA*, 2000]. Many hydrocarbon species are emitted from such sources. Understanding source impacts on urban air photochemistry requires knowledge of the particular hydrocarbon species emitted. Wide differences in reactivity with hydroxyl radical and differences in oxidation products lead to very different influences of ozone formation [*Carter*, 1994] and particulate matter formation [*Odum et al.*, 1997].

[4] Despite significant decreases in roadway CO and hydrocarbons emissions as a result of vehicle emissions controls, ozone still frequently exceeds air quality standards in many US cities [*EPA*, 2001]. The city of Houston, Texas is one such example. Over the past 10 years ozone concentrations in this area have not changed significantly despite improvements in other large metropolitan areas such as in California [*EPA*, 2001]. Houston is home to a vast petrochemical industrial complex located along the Houston Ship Channel (HSC), a 20 km waterway leading to Galveston Bay from the east side of the city. Large refineries and other petrochemical industries release a wide variety and large amounts of hyd ons and NOx. Establishing reliable hydrocarbon emission inventories for these large petrochemical complexes has been difficult owing to the various mechanisms by which hydrocarbons may be released (process vents, flares, stack emissions, cooling towers, leaky valves, etc). Understanding the relative importance of industrial emissions and roadway vehicle emissions on ozone formation in the greater Houston area will require knowledge of the hydrocarbon speciation from these sources.

[5] To better understand the chemical and meteorological factors leading to ozone formation in Houston, a large multiagency field study was conducted in August and September 2000. The Texas Air Quality 2000 study (TexAQS 2000) combined aircraft and ground based observations of ozone and its precursors. Results from aircraft measurements downwind of industrial complexes along the Ship Channel and elsewhere indicate that emissions of light alkenes and coemitted NOx from these facilities cause rapid production of ozone [*Kleinman et al.*, 2002; *Ryerson et al.*, 2003; *Daum et al.*, 2003]. This paper reports on ground based hydrocarbon measurements made at the La Porte super site during TexAQS 2000. This site was established to investigate the relative influence of petro-

chemical industry emissions and normal urban emissions attributed to road way vehicle emissions on surface ozone concentrations in Houston.

2. Experiment

[6] A wide variety of trace gas and particulate matter measurements were made at the La Porte Municipal airport during the TexAQS study. Trace gas measurements included point measurements from a 10-m tower of O_3, CO, SO_2, NO, NO_2, NOy, hydrocarbons, PANs, organic nitrates and HOx radicals, and some results have been published by *Roberts et al.* [2003], *Karl et al.* [2003] and *Rosen et al.* [2004]. Remote sensing of several trace gases by differential optical absorption spectroscopy was also performed [*Geyer et al.*, 2003]. Figure 1 shows a map of the site location depicting major roads and the largest hydrocarbon point sources. The La Porte site was located on the outskirts of a residential area and was only a block away from an elementary school. Downtown Houston was about 30 km northwest and major industrial hydrocarbon sources were about 8 km to the north along the HSC and 5 km to the south. The site was located far enough from major roads and highways that local traffic did not directly influence the measurements and provided a good representation of the combined industrial and traffic hydrocarbon emission mix that impacts Houston's air chemistry.

[7] Hydrocarbon measurements were made by four in situ instruments from 18 August to 12 September 2000. Details on the instrumentation, sampling, and the intercomparison between the measurements are described in the work of *Kuster et al.* [2004] and will only be briefly described here. The automated instruments collected and analyzed air samples for different suites of compounds. Three of the instruments were chromatography based whereby an air sample (200–500 cc) was cryogenically collected, injected onto a capillary column and separated by gas chromatography. Each in situ GC system used a different column phase and detection technique: Al_2O_3/KCl PLOT column with flame ionization detection for C_2-C_6 alkanes and alkenes (NOAA-1 instrument); HP-624 column with electron impact ion trap mass spectrometry detection for C_4-C_{10} hydrocarbons and selected C_2-C_5 aldehydes and ketones (NOAA-2 instrument); HP-624 column with electron impact quadrupole mass spectrometer detection for selected hydrocarbons and their oxidation products (University of Miami instrument). Each instrument was routinely calibrated in the field with multicomponent gas standards. The time of sample collection, sample integration time, and sampling interval was different for each instrument. The fourth instrument was a Proton Transfer Reaction Mass Spectrometer (PTR-MS) that detected selected hydrocarbons with sample integration times of seconds [*Karl et al.*, 2003]. Instruments were housed in trailers beneath a 10-m walk-up scaffold. Air was drawn down a glass manifold at $\sim$2000 L min^{-1} from the top of the scaffold to the instrument trailers where the flow was subsampled by the respective instruments. In general the level of agreement for species measured in common by these instruments was quite good [*Kuster et al.*, 2004] and the data can be combined to improve temporal coverage.

[8] Hydrocarbon samples of motor vehicle emissions were also collected in the Houston Washburn tunnel by filling 6-L SUMMA polished canisters [*McGaughey et al.*, 2004]. This tunnel passes under the HSC about 9 km northwest of La Porte. Four canisters per day with one-hour fill times were collected in the afternoon between 29 August and 1 September. Coincident with the tunnel samples, ''background samples'' were collected of the ambient air used to ventilate the tunnel. The difference in concentration between the tunnel sample and background sample was attributed to vehicle emissions. Air samples from the canisters were analyzed by GC-FID on a dual column system [*Lonneman*, 1998]. The tunnel samples are used in this paper to provide a speciated hydrocarbon roadway emissions profile.

3. Results

3.1. Time Series of Selected Hydrocarbons From La Porte

[9] Figures 2a–2c display a time series of selected hydrocarbon mixing ratios, illustrating the temporal coverage of the different instruments and the impact of apparent industrial plumes at the La Porte site. Table 1 lists the major hydrocarbons measured by the respective instruments along with observed median values and maximum values. On the basis of medians, the six most abundant hydrocarbons measured were ethane (5.9 ppbv), methanol (3.9), formaldehyde (3.9), acetone (3.7), propane (3.2), and acetaldehyde (2.5). Highest mixing ratios were observed for methanol (574), ethene (566), propene (111), and ethane (85). The most striking feature of the La Porte hydrocarbon measurements was the occurrence of extremely high mixing ratios of ethene and propene (>100 ppbv) that can only be understood as plumes from industrial emissions. In general, extended periods (hours long) of elevated ethene were associated with elevated propene and 1-butene (not shown) though mixing ratios were not well correlated suggesting independent sources. Elevated periods of light alkenes occurred on 23–25 August and 5–6 September. These increases in light alkenes were all accompanied by increases in acetylene whose principal source is thought to be roadway vehicle emissions [*Harley et al.*, 1992]. However, it will be shown in the last section of this paper that industrial emissions of acetylene are indicated. The highest ethene mixing ratios were observed as a plume on the morning of 5 September. The highest propene mixing ratio was observed as an isolated sample on 20 August in the late afternoon. Mixing ratios of other hydrocarbons did not display as much variability as ethene and propene with the exception of methanol. Most hydrocarbons displayed occasional high values, as indicated by 1,3-butadiene, i-pentane, toluene, and benzene in Figure 2b and these excursions were not typically well correlated with other hydrocarbons. For example, elevated levels of benzene observed on in the evening of 6 September (up to 28 ppbv) were not associated with elevated levels of other aromatics. This suggests an industrial source rather than vehicle emissions. Figure 2c displays the time series of selected oxygenated species. The level of agreement between the PTR-MS and NOAA-2 data for acetone and acetaldehyde was reasonable although propanal will interfere with the

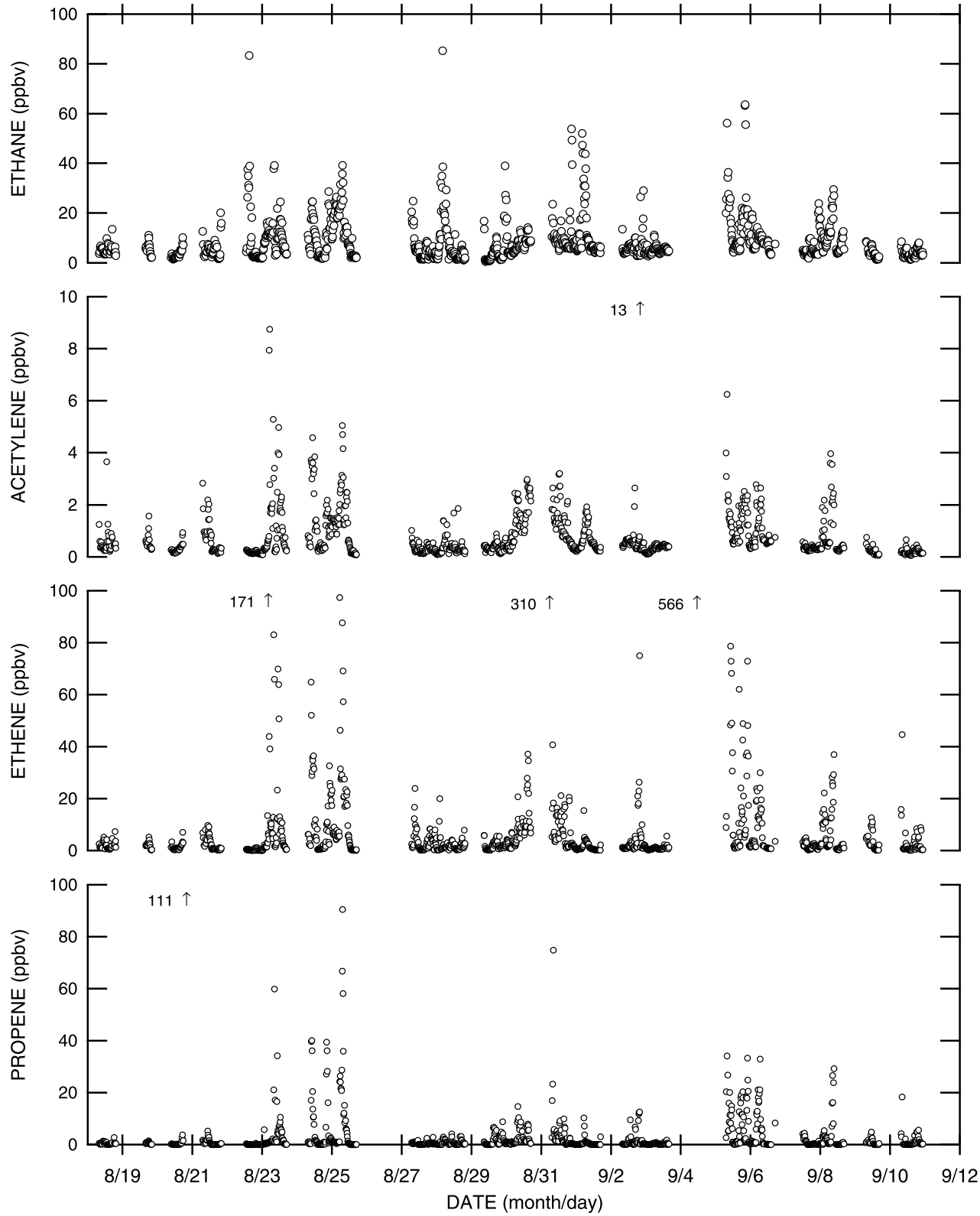

Figure 2a. Time series of selected hydrocarbon mixing ratios (ppbv) at La Porte measured by the NOAA-1 instrument. Plume data beyond scale range are indicated by arrows with corresponding maximum mixing ratio.

PTR-MS measurement of acetone. From the NOAA-2 data, propanal was about 10% of the measured acetone. Both instruments had a substantial background for acetaldehyde and were not able to ately quantify mixing ratios below about 1 ppbv. Acetaldehyde, a photoproduct of propene, displayed elevated mixing ratios during the same periods noted previously when the light alkenes were elevated. Elevated mixing ratios were also observed on

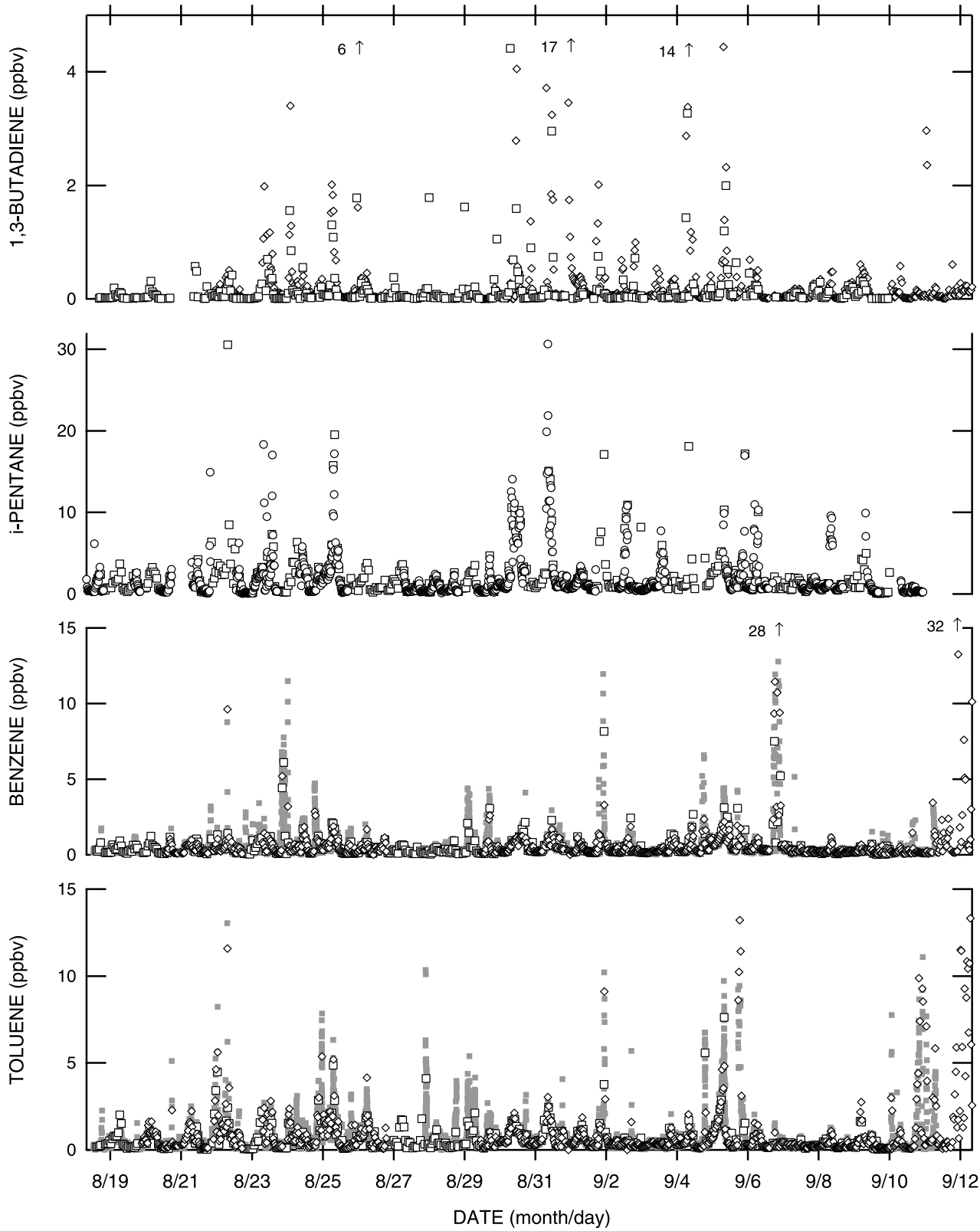

Figure 2b. Time series of selected hydrocarbons mixing ratios (ppbv) observed at La Porte. Circles are NOAA-1 instrument data, squares are NOAA-2 data, diamonds are University of Miami data, and gray dots are PTR-MS data. Plume data beyond scale range are indicated by arrows with corresponding maximum mixing ratio.

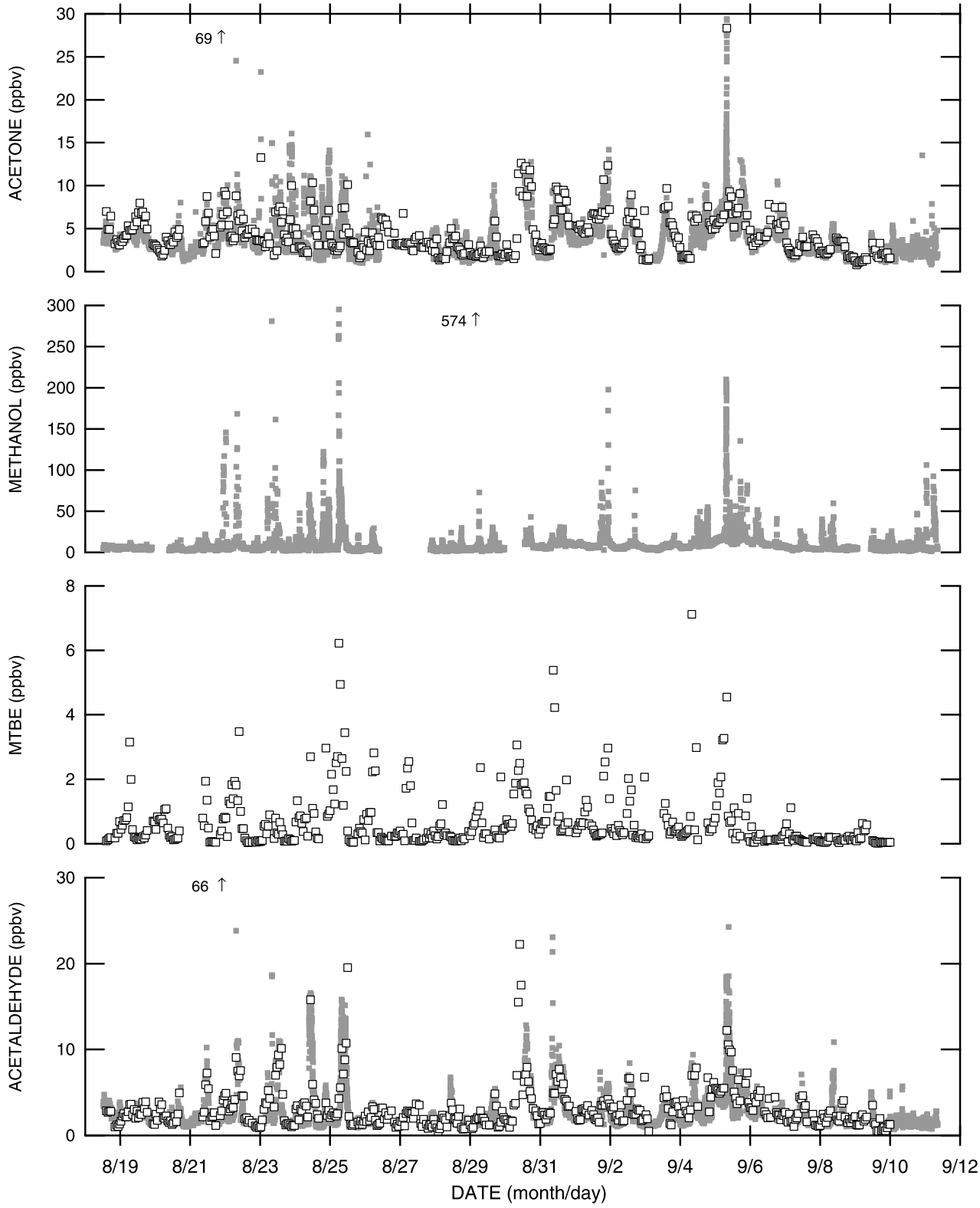

Figure 2c. Time series of selected oxygenated hydrocarbon mixing ratios (ppbv) observed at La Porte. Squares are NOAA-2 data, and gray dots are PTR-MS data. Plume data beyond scale range are indicated by arrows with corresponding maximum mixing ratio.

30–31 August, a period when ozone mixing ratios peaked at over 200 ppbv. The methanol time series is striking for the wide range in mixing ratios, implying a strong industrial influence. Methyl-tert- her (MTBE) is manufactured at refineries as an additive to gasoline. In Houston MTBE was found to comprise 10.9% by weight of gasoline composition and 6.5% by weight of the vehicle emissions measured in the tunnel [*McGaughey et al.*, 2004]. In

Table 1. Observed Median and Maximum Values at La Porte

	NOAA-1		NOAA-2		University of Miami		PTR-MS	
	1191 Samples		451 Samples		837 Samples		11241 Samples	
Species	Median, ppbV	Maximum, ppbV	Median, ppbV	Maximum, ppbV	Median, ppbV	Maximum, ppbV	Median, ppbV	Maximum, ppbV
Ethane	5.90	85.2						
Ethene	1.83	566						
Acetylene	0.41	13.2						
Propane	3.15	79.8						
Propene	0.45	111						
n-butane	1.11	18.4						
i-butane	1.21	71.6						
1-butene	0.06	41.7						
Isobutylene	0.06	3.01						
T-2-butene	0.01	0.89						
C-2-butene	0.01	1.18						
1,3-butadiene			0.052	6.48	0.087	16.7		
n-pentane			0.37	17.1				
i-pentane	0.91	30.7	1.23	30.5				
1-pentene	0.02	1.39	0.03	2.09				
Cyclopentane			0.099	46.7				
T-2-pentene	0.013	1.70	0.026	2.36				
C-2-pentene	0.009	0.98	0.016	1.43				
2-methyl-1-butene	0.021	1.52						
Isoprene	0.182	28.9	0.11	2.59	0.14	33.9		
Hexane	0.291	7.46	0.41	5.00				
2-methylpentane			0.26	3.65				
3-methylpentane	0.162	3.29	0.23	2.55				
Cyclohexane			0.090	2.51				
Heptane			0.077	0.86				
Octane			0.040	0.51				
2,2,4-trimethylpentane			0.122	1.43				
Nonane			0.020	0.37				
Deacane			0.027	0.74				
Benzene			0.34	8.16	0.321	32.1	0.34	27.7
Toluene			0.41	7.61	0.40	13.3	0.42	13.0
Ethylbenzene			0.058	2.32				
o-xylene			0.063	5.82				
m,p-xylene			0.16	11.2				
Styrene			0.013	1.47				
Isopropylbenzene			0.006	0.76				
1,2,3-trimethylbenzene			0.011	0.35				
1,2,4-trimethylbenzene			0.048	1.85				
1,3,5-trimethylbenzene			0.012	0.44				
a-pinene			0.010	0.25				
Methanol							3.90	574
MTBE			0.35	7.11				
Acetone			3.70	28.3			3.25	68.8
2-butanone			0.28	7.75				
HCHO							3.90	35.6
Acetaldehyde			2.47	22.2			1.94	66.3
Propanal			0.21	4.19				
Methacrolein					0.079	1.16		
Methyl vinyl ketone					0.129	2.26		
Acrolein					0.021	6.81		

general, mixing ratios of MTBE and toluene were similar and tracked each other fairly well. There were a couple of samples in which MTBE mixing ratios were 2 to 3 times those of toluene, suggesting that the occasional impact of an MTBE industrial source.

3.2. Mixing Ratio Frequency Distribution

[10] Hydrocarbon mixing ratio variability observed at La Porte is better illustrated in Figure 3 which displays frequency of occurrence histograms of selected alkane, alkene, and aromatic mixing ratios. Mixing ratio frequency distributions of most alkanes, most aromatics, and most of the measured olefins were reasonably lognormal. Ethene, propene, and 1-butene butions were skewed toward high mixing ratios, suggesting the influence of emission sources distinct from those of the alkanes and aromatics. Distributions of styrene and isopropylbenzene (not shown) were likewise skewed. The propane distribution appeared to be more skewed than the other light alkanes. Benzene and toluene data from the PTR-MS displayed the smoothest distributions owing to a much greater sampling frequency. In general hydrocarbon mixing ratios spanned 2 to 3 orders of magnitude.

3.3. Diel Variation

[11] Figure 4 illustrates the diel variations in local wind direction at 10 m and hydrocarbon mixing ratios. The wind direction displayed a distinct diel pattern due to the influ-

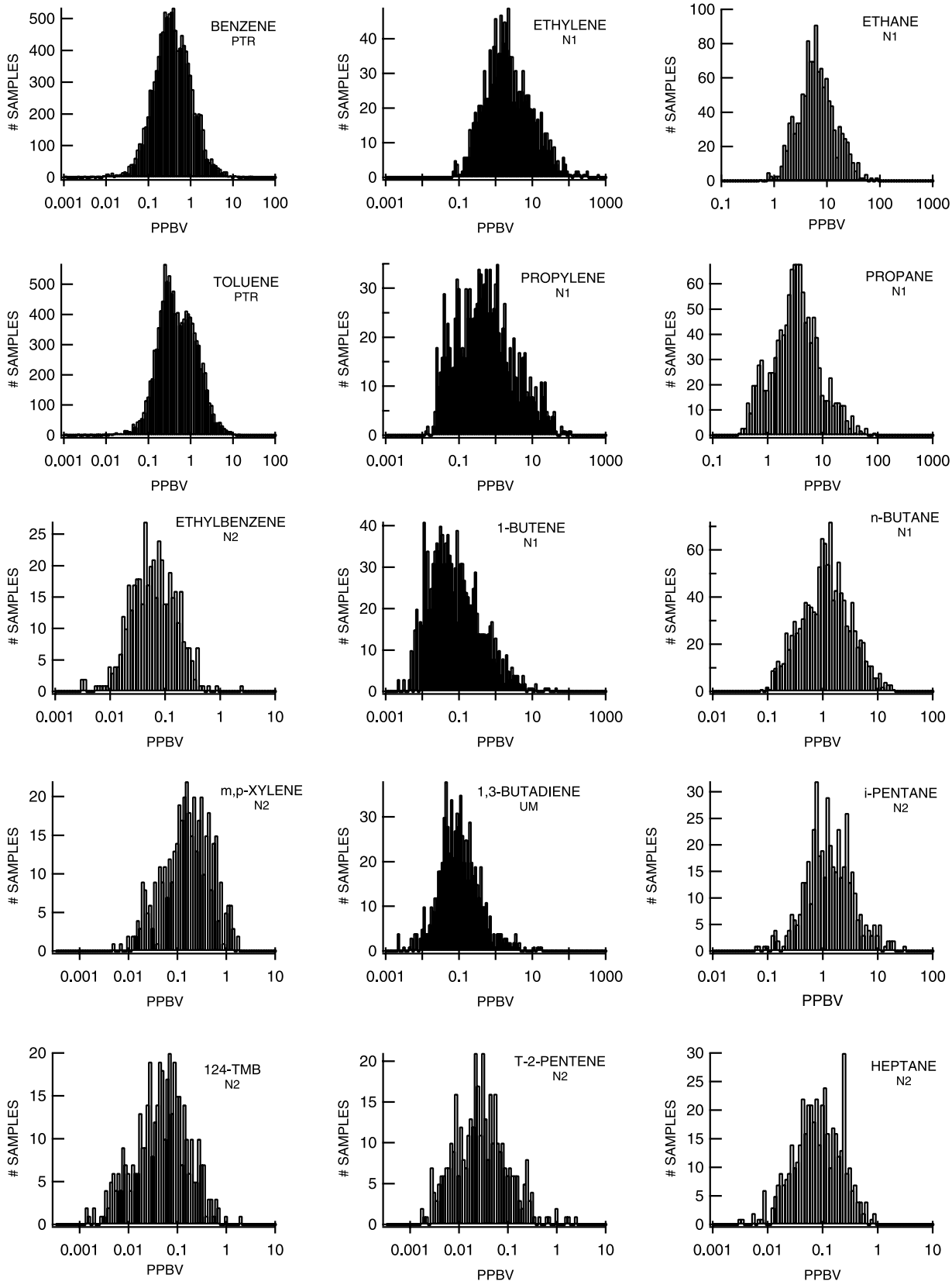

Figure 3. Histograms of selected hydrocarbons illustrating lognormal distributions for most species with the exception of ethene, propene, and 1-butene. N1, NOAA-1 data; N2, NOAA-2 data; UM, University of Miami data; and PTR, PTR-MS data.

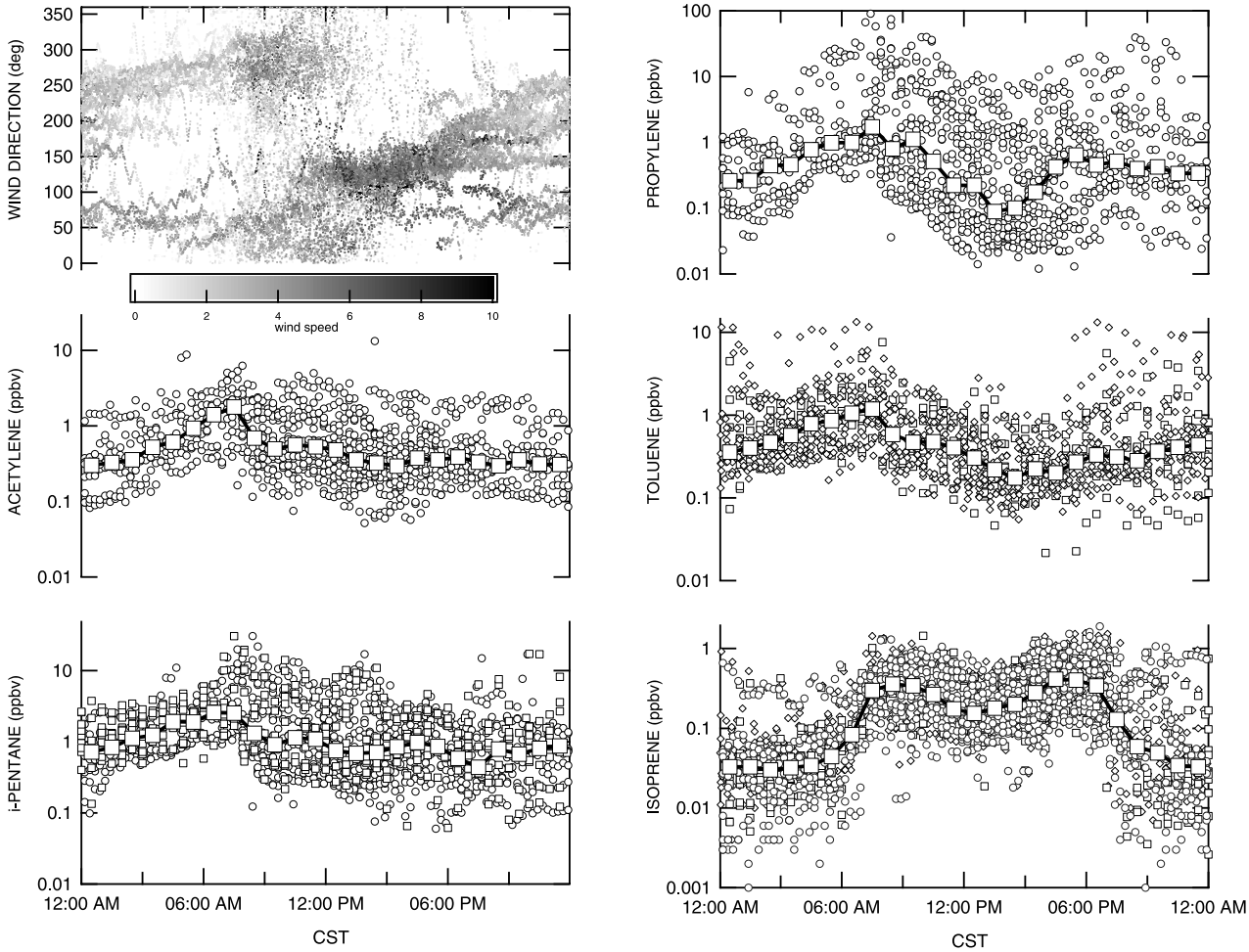

Figure 4. Diel variation of wind direction and selected hydrocarbons at La Porte, Texas. Data from the NOAA-1 instrument are shown as circles, NOAA-2 as squares, and University of Miami as diamonds. Large squares indicate hourly medians of the data shown.

ence of land-sea breeze circulations. Wind speeds were lowest in the early morning and typically highest between 1200 and 1800 CST when winds were usually from the ESE direction at 6 m s^{-1}. This pattern in wind direction and wind speed influenced hydrocarbon trends. The general pattern for hydrocarbons was a buildup during the early morning to a maximum at around 0800 followed by a decrease to a midafternoon minimum at around 1500 CST. Morning highs are consistent with typically northerly winds bringing emissions from the HSC mixed with rush hour traffic emissions, low wind speeds, small mixed layer depths, and low photochemical removal rates. The midafternoon lows are consistent with higher observed winds speeds, greater mixed layer depth and a wind direction from a relatively source free sector (Galveston Bay). More reactive hydrocarbons tended to display a more pronounced diel trend indicating that photochemical removal also contributed to afternoon lows. However, the spread in the data was similar to the diel amplitude making diel trends difficult to discern with low frequency measurements. Notably, the once per hour sampling frequency of the NOAA-2 instrument was just barely adequate to capture diel patterns that emerged from the ambient variability at La Porte. Isoprene disp a unique diel pattern featuring nonzero mixing ratios at night and a local minimum at about 1300 CST. Not shown in Figure 4 are several isoprene values >10 ppbv (max 32 ppbv) attributable to plumes from local industrial sources. Mixing ratios of isoprene during the day are likely dominated by emissions from trees that grew along the perimeter of the airport property to the north and throughout residential neighborhoods and undeveloped land in the area. The isoprene data display a transition in the morning at sunrise (~0600 CST) and sunset (~1900 CST) consistent with the sunlight dependence of biogenic emissions. *Roberts et al.* [2003] have demonstrated the local nature of the isoprene source in the daytime through parent-product reaction sequence analysis. The isoprene plumes on 24 August and nonzero nighttime mixing ratios suggest anthropogenic sources also contribute to isoprene at the La Porte site. One source of isoprene at night may be automobile emissions. Strong linear relationships between isoprene and vehicle exhaust tracers such as acetylene and 1,3-butadiene have been noted in urban areas [*McLaren et al.*, 1996; *Borbon et al.*, 2001]. The Washburn Tunnel data show isoprene in the exhaust emissions to be 0.34% of the total VOC carbon mass. Linear regressions between isoprene and exhaust tracers such as acetylene and

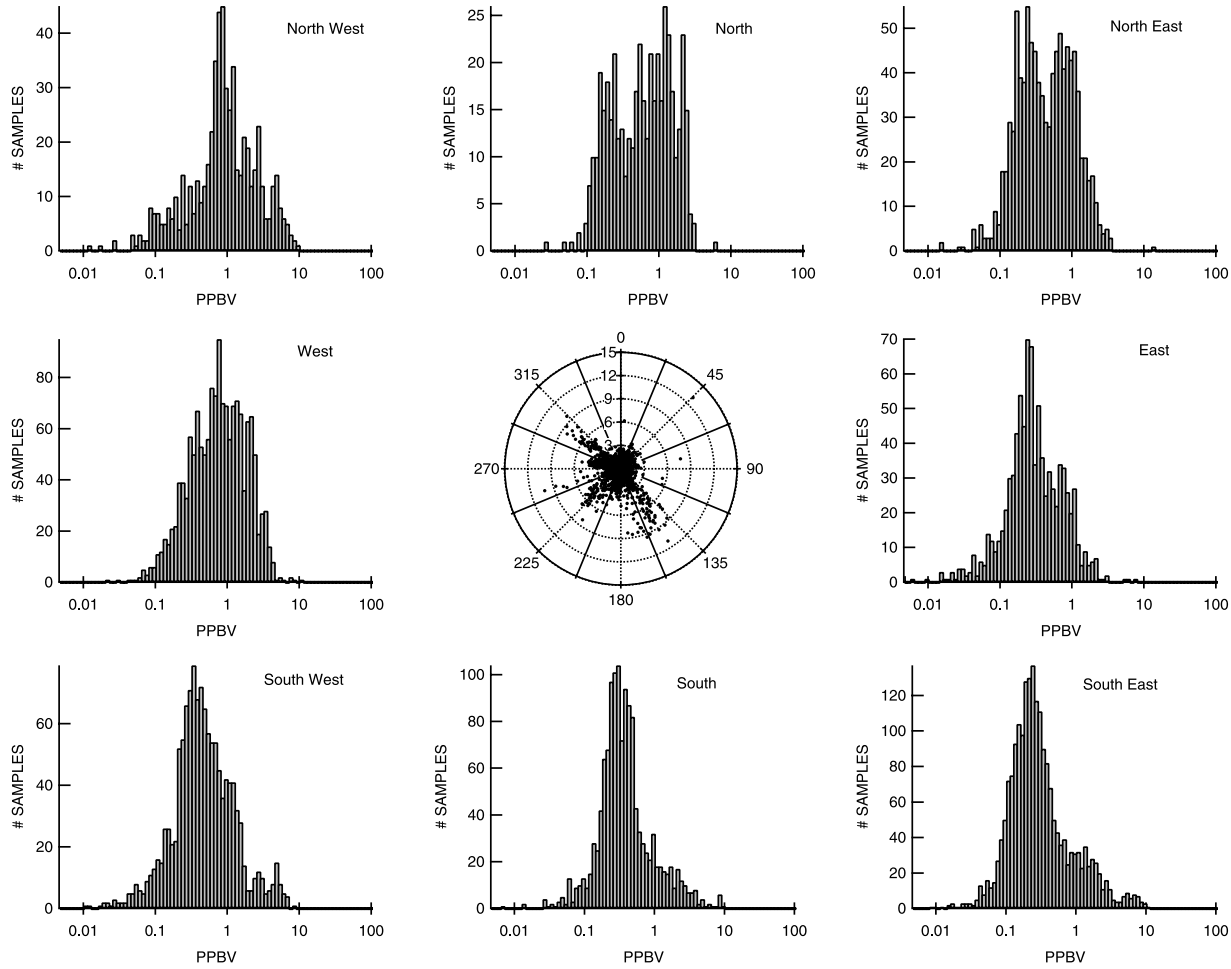

Figure 5. Toluene wind rose and mixing ratio histograms binned according to local wind direction.

1,3-butadiene measured at La Porte displayed significant scatter and much poorer correlation than those reported by *Borbon et al.* [2001]. Thus no definitive conclusions could be drawn about the nighttime isoprene source.

3.4. Wind Sectored Histograms

[12] To better understand the influence of potential industrial emissions of ambient mixing ratios at La Porte, data were binned according to local wind direction and histograms plotted. The large amount of continuous data collected from the PTR-MS (>11,000 samples) allowed good statistical sampling and clear wind sectored trends. The sectored toluene data from the PTR-MS are shown in Figure 5. Highest toluene mixing ratios were observed for the southern sectors and from the north west sector. The north west sector would be impacted by HSC emissions, while the southern sectors appeared to be impacted by the small cluster of industries illustrated in Figure 1. Most sectors display a mode centered between 0.20 and 0.35 ppbv which we term a local background for toluene. The west sector displayed higher mixing ratios centered around 0.9 ppbv, which may reflect the impact of traffic emissions since western winds typically occurred in the mid morning.

[13] The wind sectored histograms for ethene are shown in Figure 6. Despite the nearly 1200 samples collected during the study period the samples were perhaps too few to draw definitive conclusions about wind sectored statistical distributions. However some interesting differences from the toluene distributions are apparent. Highest ethene mixing ratios (>100 ppbv) were most often observed from the northwest sector. While this sector would bring emissions from the Houston city center it could also bring emissions from the large refinery complex at the west end of the HSC (Lyondell-Citgo) depicted in Figure 1. Interestingly, all sectors had samples with ethene >10 ppbv including the east sector that encompasses Galveston Bay. The southern and west sector histograms display a mode at around 1–2 ppbv ethene The wind sectored propene distributions (not shown) were somewhat similar to that of ethene; high mixing ratios making up the tail of the distribution (>10 ppbv) occurred in all wind sectors. The highest mixing ratio (111 ppbv) came from the south east sector. The distribution of elevated ethene mixing ratios among all sectors despite large point sources being located in the north is likely a result of land sea breeze circulation patterns. Back trajectories determined from a network of wind profilers [*Berkowitz et al.*, 2004] show that afternoon

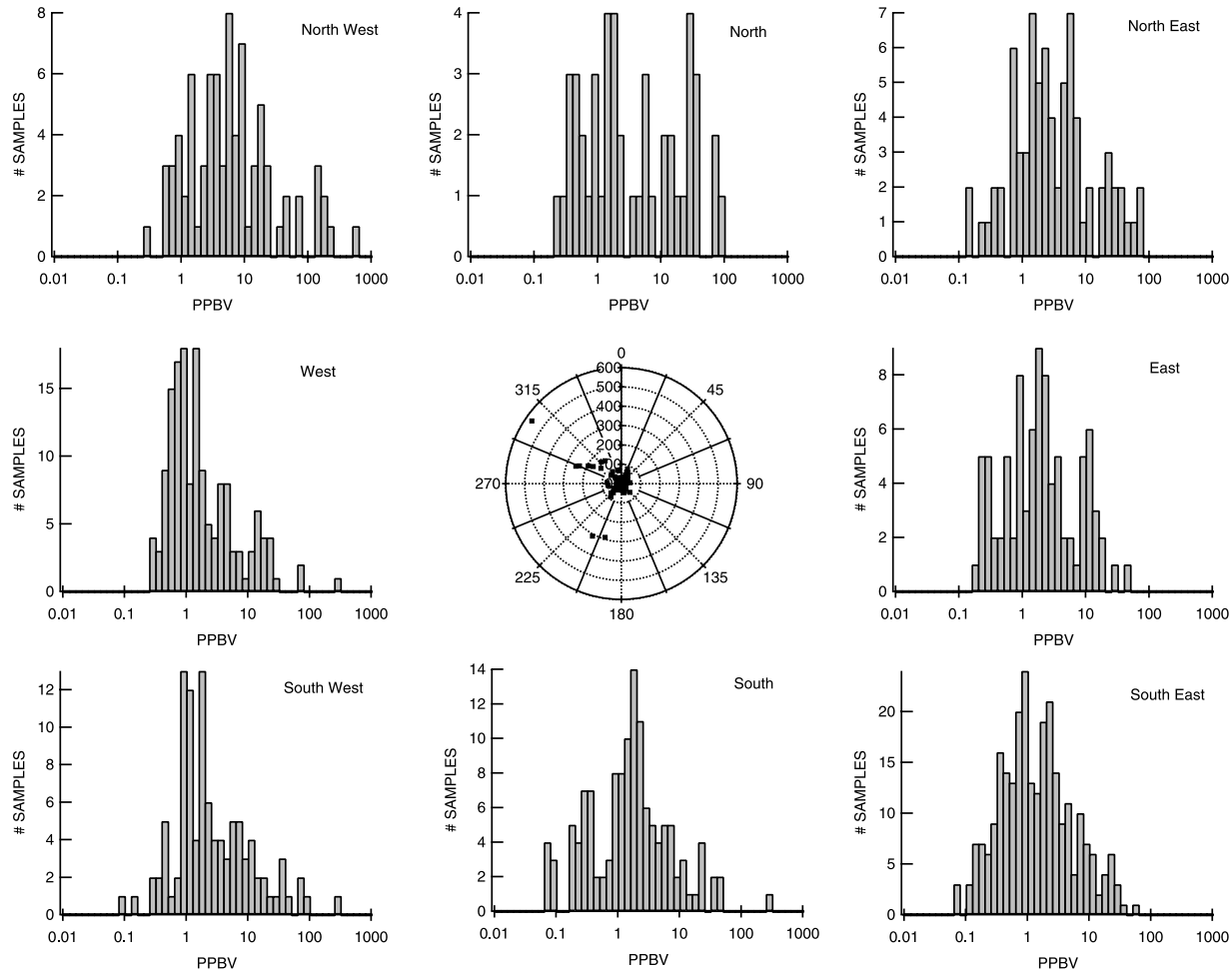

Figure 6. Ethene wind rose and mixing ratio histograms binned according to local wind direction.

winds from the south may well be bringing emissions from the HSC. Thus using local wind direction to apportion plumes to source locations may have limited applicability in the Houston metropolitan region.

3.5. Comparison of La Porte Data to Vehicle Exhaust Signature

[14] Since roadway vehicle emissions are a dominant hydrocarbon source in urban areas [*Watson et al.*, 2001; *Choi and Ehrman*, 2004], the vehicle exhaust source signature from the Washburn Tunnel samples was compared with the La Porte data to better understand the impact of industrial emissions on the measured hydrocarbon distributions. To remove the impact of photochemical aging on source signatures, regressions were made between species with similar atmospheric lifetimes. The source ratio is preserved for species with similar lifetimes because photochemical loss and mixing will result in similar rates of concentration change [*Parrish et al.*, 1998; *Jobson et al.*, 1999]. Thus all the data could be plotted, including data from the afternoon when mixing ratios were typically lower due to mixing and photochemical removal. The slope defined by the ambient data defines the source ratio that can be directly compared to the Washburn Tunnel data and literature values. In pra there are a limited number of species that can be plotted and we have constrained the hydrocarbon pairings such that removal rates due to reaction with HO are not different by greater than 20%. The exception in this analysis is the regression between propene and ethene.

[15] Correlations between selected alkenes are shown in Figure 7. In addition to the La Porte and Washburn Tunnel data an average vehicle exhaust molar ratio is also shown calculated from published tunnel sampling of light duty vehicles from six studies conducted in the 1990s [*Conner et al.*, 1995; *Kirchstetter et al.*, 1996; *Sagebiel et al.*, 1996; *Fraser et al.*, 1998; *Rogak et al.*, 1998]. The average ratio from the tunnel sampling studies, the Washburn Tunnel data, and the median ratio observed at La Porte are tabulated in Table 2. For t-2-pentene versus c-2-pentene there is excellent agreement between the Washburn Tunnel data, the literature, and the ambient data. The ambient mixing ratios span 3 orders of magnitude driven by atmospheric processing and variations in source strength. The very tight correlation and good agreement with the exhaust emissions ratio serves as a benchmark example in this analysis of a clear vehicle exhaust source signature. The t-2-butene versus c-2-butene also displays a good correlation and reasonable agreement with the vehicle exhaust ratios, although the median ratio at La Porte is slightly lower (0.88) than that

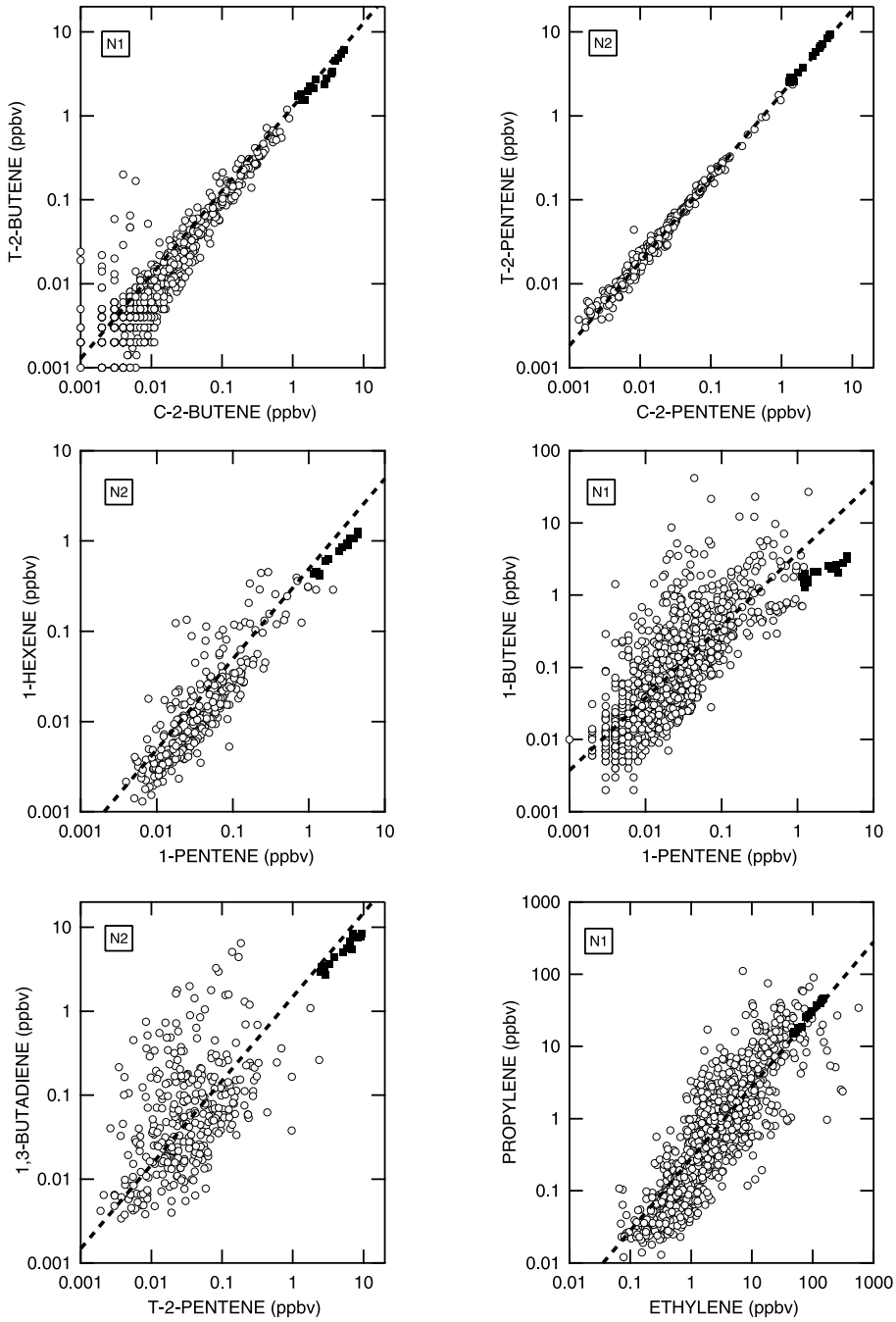

Figure 7. Correlations between alkenes comparing La Porte data (open circles) to Washburn Tunnel samples (squares) and average vehicle exhaust ratio from the literature (dashed line). N1 indicates NOAA-1 data, and N2 indicates NOAA-2 data.

found in Washburn Tunnel (1.13 ± 0.18). With the exception of a few high t-2-butene values at low c-2-butene mixing ratios, the good correlation and level of agreement with the tunnel samples also suggests that the major source of these species was vehicle exhaust. For 1-hexene versus 1-pentene the bulk of the La Porte data (median = 0.29) are in good agreement with the Washburn Tunnel data (average = 0.32 ± 0.04), with the average from the other tunnel studies giving a slight higher ratio (0.49 ± 0.25). There were occasional high values of 1-hexene but t ta trend suggests 1-hexene and 1-pentene were primarily from vehicle exhaust emissions. In contrast is the plot between 1-butene and 1-pentene where there is poor agreement between the La Porte data, the Washburn Tunnel data, and the single reported literature ratio from *Kirchstetter et al.* [1996]. The La Porte data display markedly elevated 1-butene mixing ratios, frequently higher than those observed in the tunnel. The Washburn Tunnel data (average = 1.03 ± 0.30) define a lower bound to the La Porte data (median = 3.09). We conclude from this plot that 1-butene levels are significantly impacted by

Table 2. Hydrocarbon Molar Ratios Measured at La Porte and in Vehicle Exhaust Studies

	La Porte	Washburn Tunnel		Vehicle Exhaust Studies	
Alkene Ratios	Median	Average	Standard Deviation	Average	Standard Deviation
t-2-butene/c-2-butene	0.88	1.13	0.18	1.27	0.33
t-2-pentene/c-2-pentene	1.90	1.91	0.09	1.78	0.19
1-hexene/1-pentene	0.29	0.32	0.04	0.49	0.25
1-butene/1-pentene	3.09	1.03	0.30	3.75	na
1,3-butadiene/t-2-pentene	1.50	1.06	0.16	1.36	0.51
Propene/ethene	0.22	0.31	0.01	0.30	0.04
Alkane Ratios					
i-butane/n-butane	1.03	0.18	0.02	0.19	0.08
i-pentane/n-pentane	3.36	3.25	0.16	2.97	0.57
2-methylpentane/3-methylpentane	1.20	1.57	0.03	1.69	0.11
Hexane/2-methylpentane	1.25	0.60	0.02	0.52	0.05
Cyclohexane/heptane	0.98	0.27	0.03	0.43	0.17
Octane/nonane	1.80	1.86	0.21	1.49	0.05
Aromatic Ratios					
Toluene/benzene	1.41	2.00	0.14	1.59	0.28
Ethylbenzene/toluene	0.14	0.16	0.014	0.17	0.027
Iisopropyl/benzene/toluene	0.011	0.015	0.002	0.02	0.008
o-xylene/m,p-xylene	0.37	0.38	0.019	0.38	0.019
Styrene/1,3,5-trimethylbenzene	1.09	0.72	0.18	0.81	0.21
1,2,3-trimethylbenzene/1,2,4-trimethylbenzene	0.23	0.24	0.015	0.25	0.07

sources other than vehicle exhaust, likely emissions from the petrochemical industry. Similarly 1,3-butadiene displayed a poor correlation with t-2-pentene with 1,3-butadiene mixing ratios tending to be above the vehicle exhaust source ratio line. The propene versus ethene plot also displays considerable scatter. The vehicle exhaust emissions ratio (0.30) bisects the data, but the large amount of scatter about this ratio (two orders of magnitude) is indicative of multiple independent sources, i.e., sources and emissions rates of propene are not strongly correlated with sources and emission rates of ethene. Compared to the other plots a significant fraction of the ambient data is at a higher concentration than the Washburn Tunnel data, another indication of strong source in addition to vehicle exhaust. The propene versus ethene plot violates the basic condition of this analysis since propene is about 3 times more reactive toward HO than ethene and the ratio would decrease with atmospheric processing.

[16] Correlations between selected alkanes are shown in Figure 8. The most obvious deviation form a vehicle exhaust signature was observed for the i-butane versus n-butane ratio, where the La Porte data show a ratio of about 1 compared to an average for the Washburn Tunnel of 0.18 ± 11%, and reported average exhaust ratio range of 0.19 (range 0.10 to 0.27) shown in Table 2. The higher i-butane to n-butane ratio at La Porte might be due to emissions from natural gas feed stocks for the petrochemical industry. A Texas refinery emissions profile reported by *Watson et al.* [2001] has i-butane/n-butane ratio >100. Ratios of i-butane to n-butane measured in other urban and remote locations were typically around 0.5 [*Jobson et al.*, 1998] and it is interesting that this ratio is typically 3 times larger than the roadway exhaust ratio. This suggest that the butanes have major sources other than roadway vehicle exhaust. Gasoline composition in Houston, averaged across brands and s, had an i-butane to n-butane ratio of 0.15 ± 0.07. *Conner et al.* [1995] have previously reported that i-butane to n-butane ratios in whole gasoline and in gasoline headspace vapors have values comparable to roadway emissions. Raw gasoline spillage and headspace vapors can not explain ratios i-butane to n-butane ratios $\geq$0.5. The impact of natural gas emissions may be important but there are surprising few data of speciated commercial natural gas profiles. *Fujita* [2001] report an i-butane to n-butane ratio of 0.60 for CNG used in Cuidad Juarez, Mexico and *Mayrsohn et al.* [1977] reported a CNG value of 0.68 for samples collected in California during the 1970s. Notable deviations from the vehicle exhaust ratio were also observed for hexane and cyclohexane. To a lesser extent octane appeared to be impacted by industrial emissions as well.

[17] Of the aromatic species isopropylbenzene and styrene displayed significant scatter suggesting the importance of industrial sources as illustrated in Figure 9. The xylenes and trimethylbenzenes showed reasonably good agreement with vehicle exhaust ratios. The plot between ethylbenzene and toluene was also in good agreement although the data more scattered. It has already been noted that toluene mixing ratios appear to be occasionally impacted by emissions from the HSC and industries to the south, but these tend to be brief occurrences and industrial plumes have not impacted its distribution significantly as sampled by the NOAA-2 instrument. The toluene versus benzene plot violates our assumptions of similar reactivity but is shown to illustrate the benzene variability and more frequent impact of elevated benzene mixing ratios. Toward the end of the experiment the PTR-MS and University of Miami instruments observed frequent benzene and toluene plumes, and as a result display much more scatter than shown in Figure 9. The caveat must be made that conclusions regarding source impacts at this site have limited generalization given the apparent temporal variability of industrial emissions.

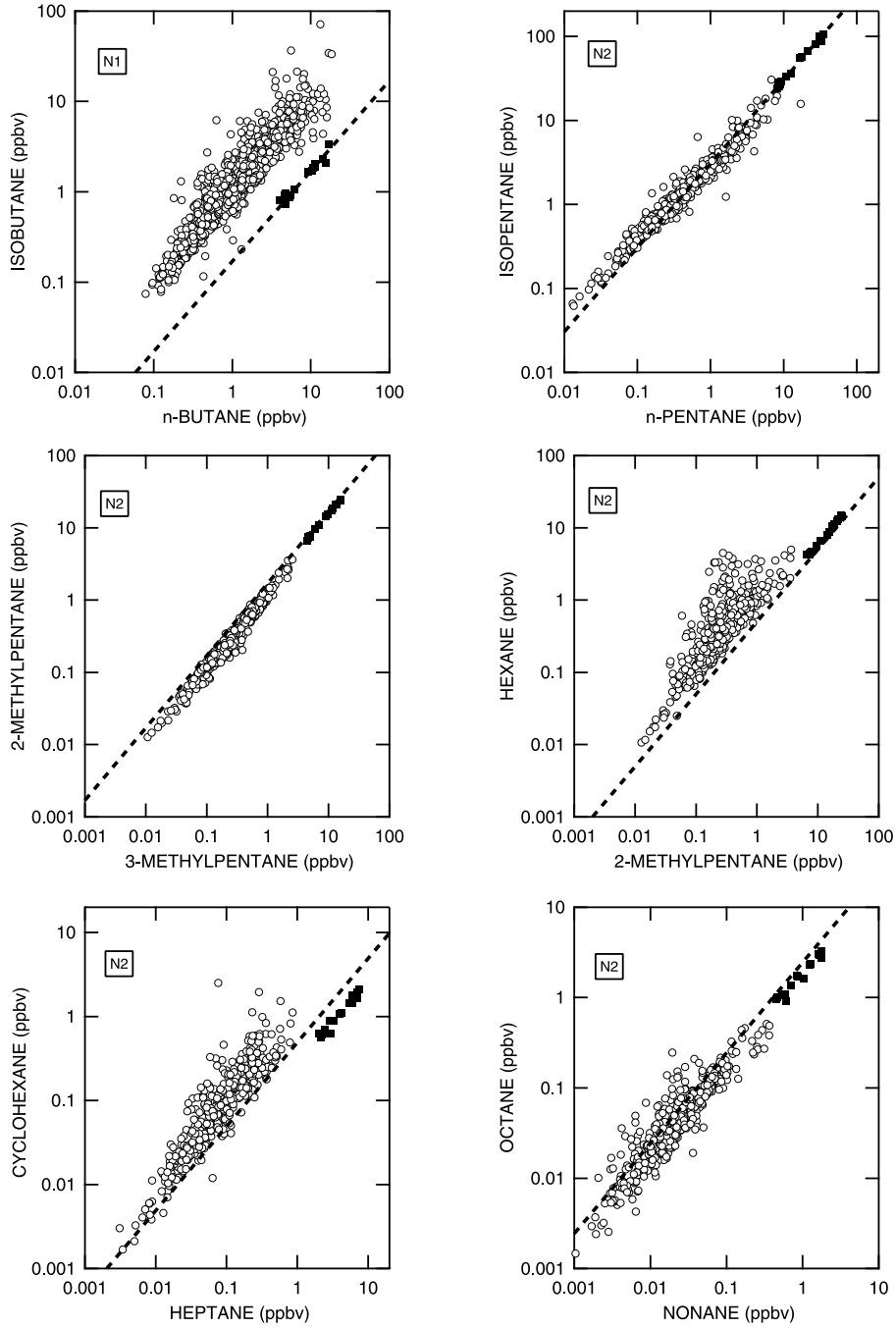

Figure 8. Correlations between alkanes comparing La Porte data (open circles) to Washburn Tunnel samples (squares) and average vehicle exhaust ratio from the literature (dashed line). N1 indicates NOAA-1 data, and N2 indicates NOAA-2 data.

[18] Another method of comparing the ambient data to the roadway vehicle exhaust signature is to compare ratios using a particular species as a reference. Acetylene is often used as a vehicle exhaust tracer to which the abundances of other hydrocarbons are compared. In this case we compared hydrocarbon abundances relative to i-pentane since this was measured by both the NOAA-1 and NOAA-2 instruments allowing the two data sets to be combined to cover the C_2-C_{10} range. Isopentane was the dominant hydrocarbon measured e Washburn Tunnel samples comprising 7.7% by weight of the hydrocarbon emissions [*McGaughey et al.*, 2004] and thus is a good tracer of vehicle exhaust. Using ratios normalizes the large difference in concentrations that exist between the two environments and will enable a direct comparison of hydrocarbon distribution patterns. To mitigate changes in ratios that can occur in transport due to chemical removal, the La Porte data were restricted to the morning period between 5 AM and 9 AM CST. This would be a period of low photochemical activity, since HO and O_3 oxidation rates were at their lowest, and the

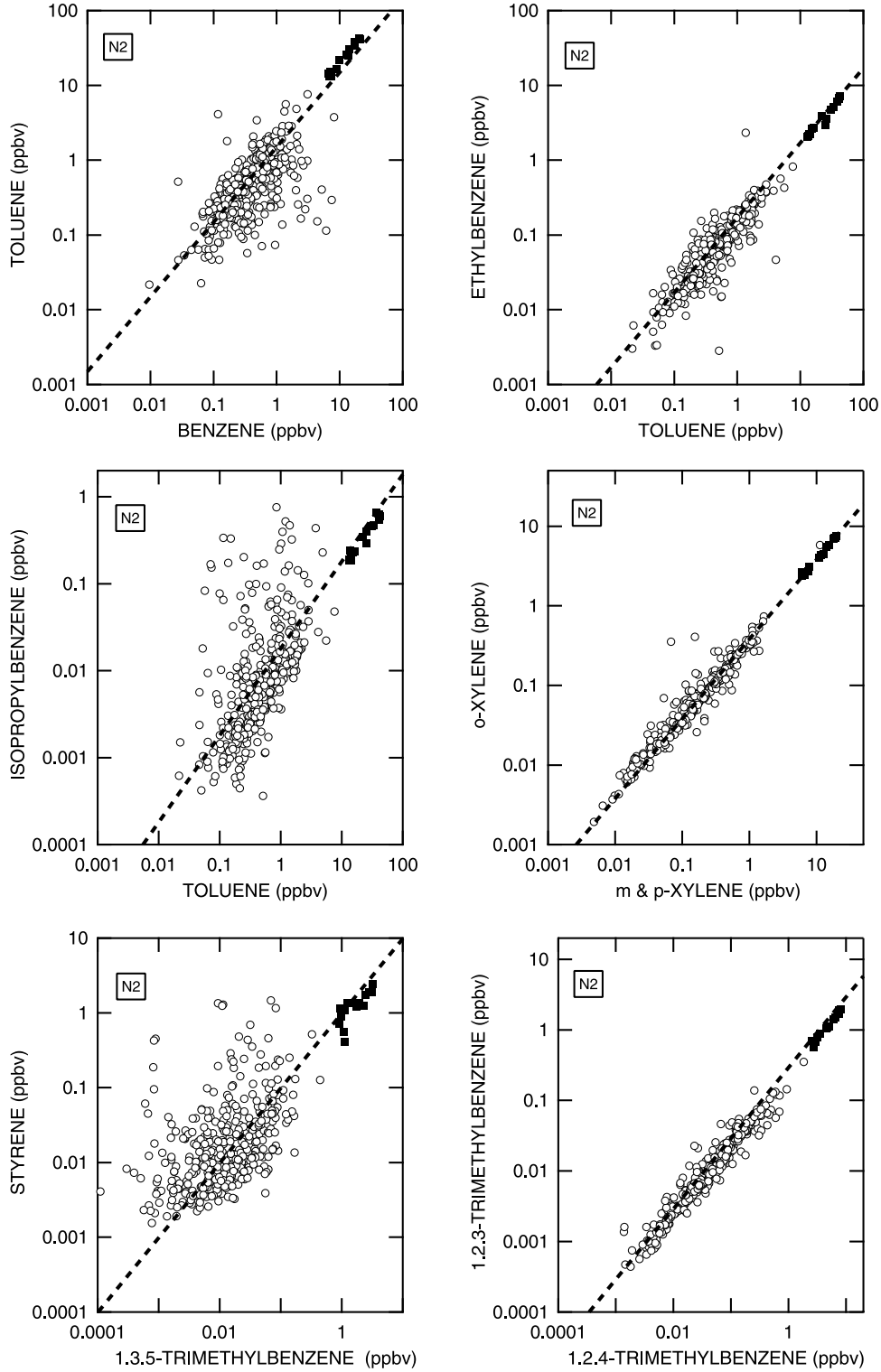

Figure 9. Correlations between aromatics comparing La Porte data (open circles) to Washburn Tunnel samples (squares) and average vehicle exhaust ratio from the literature (dashed line). All ambient data are from the NOAA-2 instrument.

source ratio better preserved. It is also a period when hydrocarbon ratios were at their highest. This period of the day is typically used for chemical mass balance analysis of source impacts [*Watson et al.*, 2001]. Midmorning hydrocarbon data displ wide range of mixing ratios, some species varied over 3 orders of magnitude, producing very skewed frequency distributions of the hydrocarbon-to-isopentane ratio. For this reason median values of the hydrocarbon-to-isopentane ratio were compared and are displayed in Figure 10 along with the 10th and 90th percen-

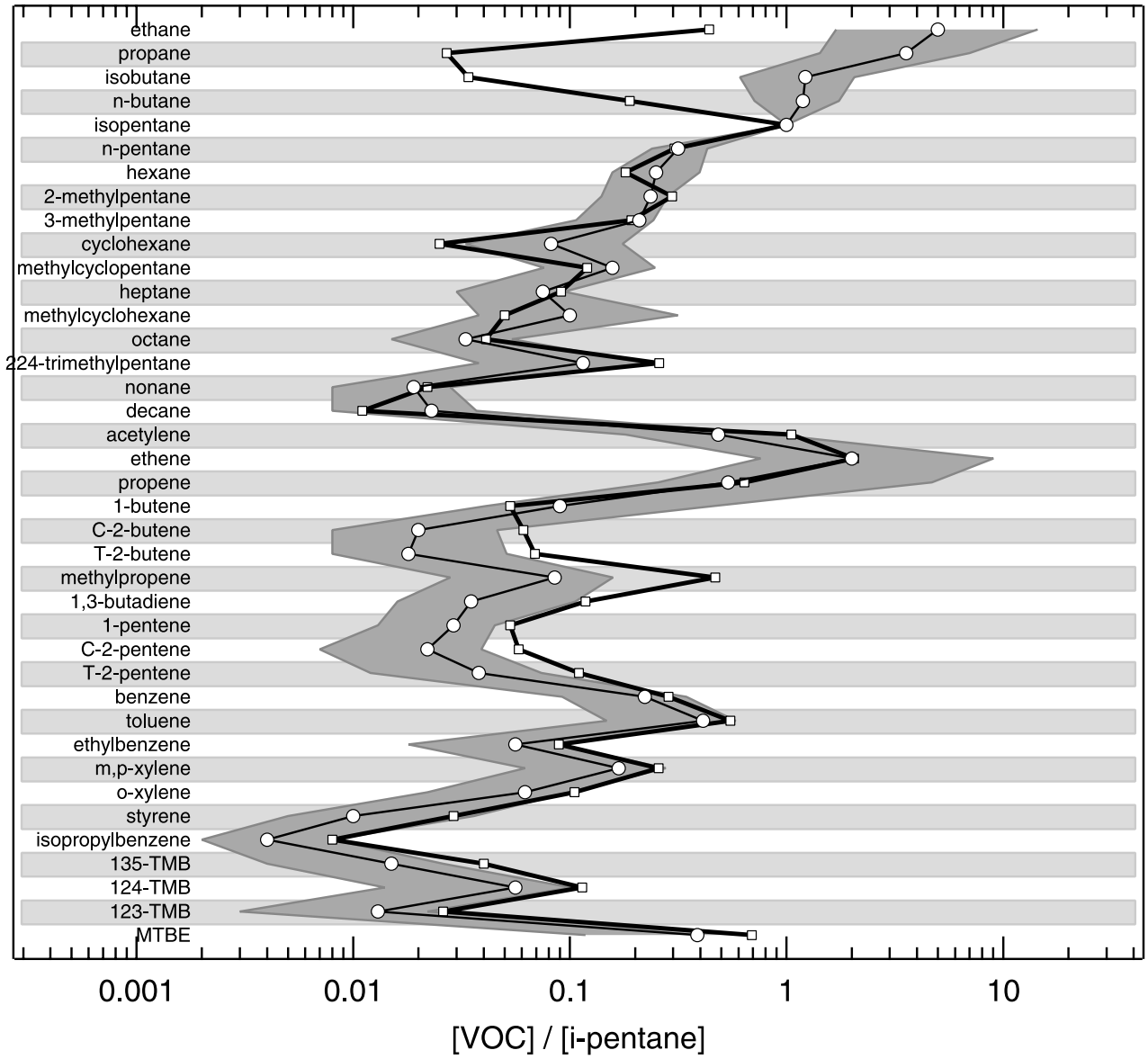

Figure 10. Comparison of La Porte and Washburn Tunnel hydrocarbon abundances relative to i-pentane. Shown are the median tunnel values (squares) and median values from La Porte for data collected between 0500 and 0900 CST (circles) bounded by the 10th to 90th percentile values (shading).

tile ranges. Overall the relative distribution at La Porte is similar to the exhaust pattern with a few notable exceptions. It is apparent in the La Porte data that species that are more reactive with HO displayed a bigger deviation from the exhaust ratio suggesting a chemical aging bias in the data. Very reactive species such as the C_4-C_5 alkenes whose HO reaction rates are at least 8 times those of i-pentane, had median ratios that were about 30% of the exhaust values. For example, while the abundances of c-2-pentene and t-2-pentene relative to i-pentane at La Porte were 37% and 34% those of the tunnel samples, the correlation between c-2-pentene and t-2-pentene displayed in Figure 7 was in excellent agreement with the exhaust ratio. This discrepancy is due to chemical aging; cis and trans 2-pentene are about 17 times more reactive O than i-pentane. These data clearly illustrate limitations in using chemical mass balance modeling of source profiles to ascribe source contributions of reactive hydrocarbons. Notable exception to the alkene loss is 1-butene whose relative abundance at La Porte was greater than the exhaust values instead of much less, consistent with our conclusions drawn from the previous analysis that industrial sources of 1-butene were significant.

[19] Very large departures from the tunnel data were observed for C_2-C_4 alkanes. These species are less reactive than i-pentane and chemical aging would increase their ratios relative to the source ratio. The largest deviation was for propane, observed to be 132 times more abundant at La Porte, followed by i-butane at 36 times, ethane at 11, and n-butane at 6.3. Isopentane is about 15 times more reactive than ethane, and given the differences that were

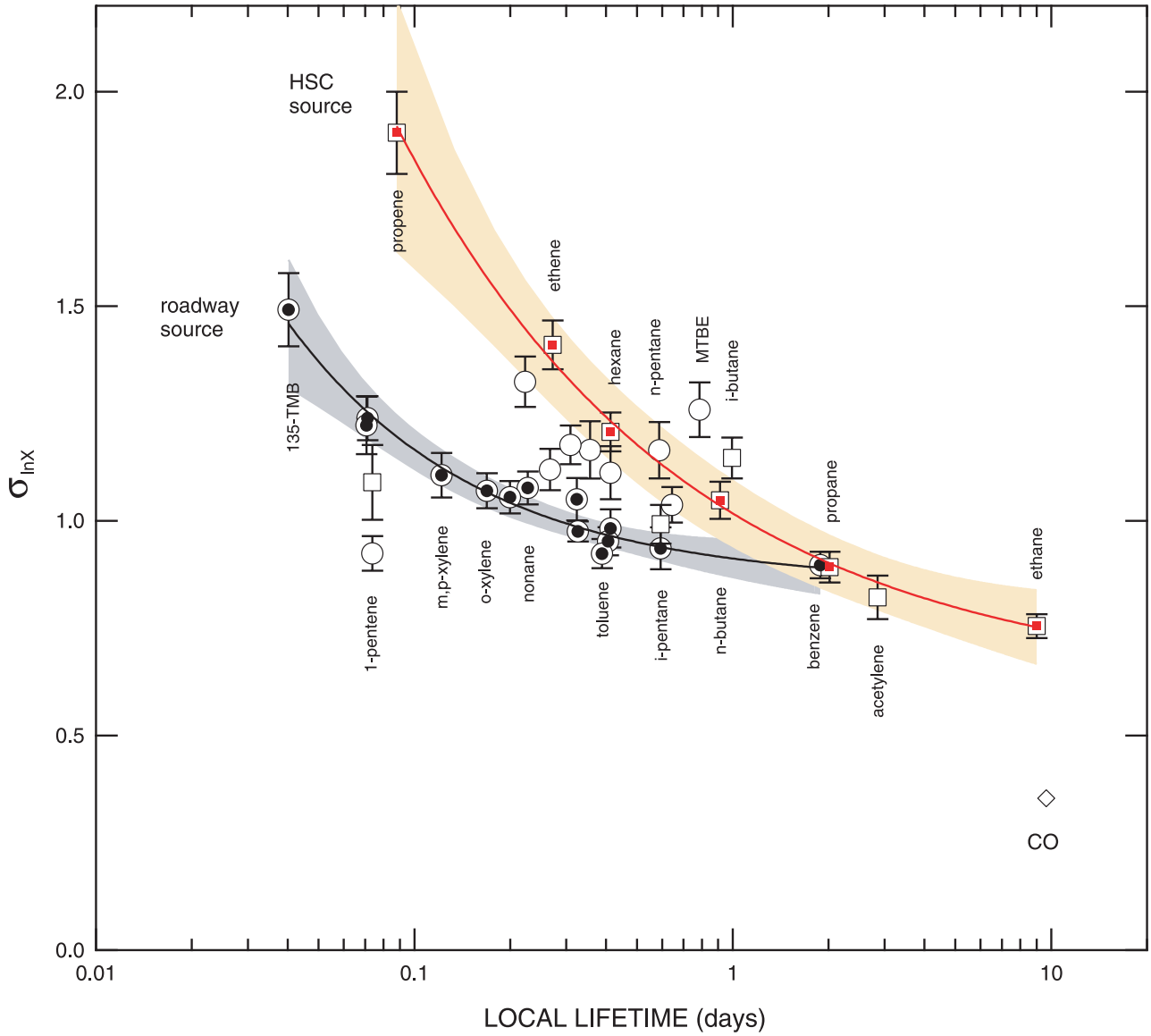

Figure 11. Relationship between the standard deviation of $\ln(X_i)$ and lifetime. Square symbols are data from the NOAA-1 instrument, and circles represent data from the NOAA-2 instrument. Black filled symbols were species whose relative abundances were consistent with a roadway vehicle emissions source and have been fitted by a power law trend. Red filled symbols were species identified to be dominated by industrial emissions and have been fitted by a power law trend. Shaded area represents the 95.5% confidence interval of the respective power law fits to the data.

seen for the cis and trans 2-pentene ratios, it could be anticipated that La Porte ethane/i-pentane ratio would be ~1.1, similar to its source ratio. The observed ratio of 11 suggests ethane is dominated by emission sources other than roadway exhaust. The butane isomer HO rate constants are about 60% those of i-pentane while propane is 30% as reactive, and their very large deviations can not be explained by chemical aging. Roadway vehicle emissions appeared to be a minor source term in the C_2-C_4 alkane budgets. Possible sources would be natural gas or other gas feedstocks used by the petrochemical industry. Cyclohexane and methylcyclohexane were factors of 3 and 2 more abundant at La Porte. Toluene and the larger aromatics displayed lo tios that the tunnel samples, consistent with an aging biases, but interestingly the 90th percentile data agreed very well with the tunnel data. The 90th percentile data perhaps reflects fresher emissions and less aging bias. Surprisingly the ethene and propene median ratios were very similar to their relative abundance in exhaust, but a very wide range of values was observed at La Porte, with 90th percentile values 4.5 times greater than the exhaust ratio.

3.6. Relationship Between Hydrocarbon Mixing Ratio Variability and Reactivity

[20] It has been observed that the spatial and temporal variability of hydrocarbon mixing ratios display an inverse power law relationship to atmospheric lifetime (τ) for rural

Table 3. Variability Data[a]

NOAA-1 Species[b]	$k_{HO} \times 10^{-12}$ cm^3 molecule^{-1} s^{-1}	σ
Ethane	0.257	0.755 ± 0.028
Acetylene	0.812	0.822 ± 0.050
Propane	1.15	0.892 ± 0.036
i-butane	2.33	1.147 ± 0.048
n-butane	2.54	1.048 ± 0.043
i-pentane	3.9	0.992 ± 0.045
Hexane	5.61	1.207 ± 0.045
Ethane	8.52	1.411 ± 0.057
Propene	26.3	1.904 ± 0.095
1-pentene[c]	31.4	1.092 ± 0.087
NOAA-2 Species[b]	**$k_{HO} \times 10^{-12}$ cm^3 molecule^{-1} s^{-1}**	**σ**
Benzene	1.23	0.897 ± 0.031
Methyl-tert-butyl ether	2.94	1.259 ± 0.064
2,2,4-trimethylpentane	3.59	1.037 ± 0.042
i-pentane	3.9	0.936 ± 0.049
n-pentane	3.94	1.165 ± 0.065
2-methylpentane	5.6	0.982 ± 0.044
hexane	5.6	1.112 ± 0.062
3-methylpentane	5.7	0.953 ± 0.033
Toluene	5.96	0.924 ± 0.034
Isopropylbenzene	6.5	1.165 ± 0.067
Ethylbenzene	7.1	0.975 ± 0.023
n-heptane	7.15	1.050 ± 0.049
cyclohexane	7.49	1.177 ± 0.045
n-octane	8.68	1.118 ± 0.048
n-noane	10.2	1.077 ± 0.038
Methylcyclohexane	10.4	1.324 ± 0.059
n-decane	11.6	1.055 ± 0.038
o-xylene	13.7	1.070 ± 0.041
p,m-xylene	19	1.106 ± 0.052
1-pentene[c]	31.4	0.924 ± 0.040
1,2,4-trimethylbenzene	32.5	1.239 ± 0.051
1,2,3-trimethylbenzene	32.7	1.223 ± 0.067
1,3,5-trimethylbenzene	57.5	1.492 ± 0.086

[a]Rate constants from *Atkinson* [1994].
[b]Italicized species were not included in power law fits.
[c]Dynamic range not quantified, ~10% data below detection limits.

and remote environments [*Jobson et al.*, 1998; *Ehhalt et al.*, 1998; *Colman et al.*, 1998; *Jobson et al.*, 1999; *Williams et al.*, 2000, 2001; *Karl et al.*, 2001]. Frequency distributions of hydrocarbon mixing ratios in these environments also appear to be lognormal, in particular for reactive species [*Jobson et al.*, 1999]. Chemical transport modeling studies have shown that species with similar source distributions and removal mechanisms define coherent variability-lifetime trends [*Hamrud*, 1983; *Ehhalt et al.*, 1998; *Johnston et al.*, 2002]. *Lenschow and Gurarie* [2002] have reviewed theoretical treatments and presented an analytical diffusion model as a conceptual framework for understanding the physical basis of variability lifetime relationships in the troposphere. Observations of temporal variability at a fixed sampling location in remote areas show that anthropogenic hydrocarbon variability is typically proportional to $\tau^{-0.5}$ [*Jobson et al.*, 1999; *Williams et al.*, 2001; *Karl et al.*, 2001].

[21] In an urban environment much of the hydrocarbon mixing ratio variability is likely due to variations in emissions and their subsequent dispersion into varying mixed layer depths and strong variability-lifetime dependence would not be anticipated. Suburban environments, like La Porte, where a wider range of processed air mass histories is possible, may reveal coherent trends. Of the species measured at La Porte, omatics displayed reasonably lognormal frequency distributions and results from section 5 indicate that automotive exhaust is likely the dominant source of these species, at least according to the time periods sampled by the NOAA-2 instrument. Exceptions were isopropylbenzene, styrene, and to a lesser extent benzene. A number of alkanes also appear to be principally vehicle exhaust constituents, and like the aromatics, are principally removed from the atmosphere by reaction with HO. The C_2-C_4 alkanes, ethene, propene and 1-butene appear to be strongly impacted by industrial emissions and therefore have a source distribution different than that of the vehicle exhaust constituents. It is anticipated that two distinct variability-reactivity trends would be defined by these data.

[22] Hydrocarbon variability for the NOAA instrument data was calculated from lognormal regressions to mixing ratio frequency distribution histograms. The histograms where fit by the log normal probability density function expression

$$y = y_o + A \times \exp\left[-\left[\frac{\ln(x/x_0)}{\sqrt{2}\sigma}\right]^2\right]. \quad (1)$$

The value of σ obtained from the fit (the standard deviation of ln(χ) where χ is the mixing ratio) was plotted versus local lifetime in Figure 11. Local lifetimes were calculated assuming an average HO concentration of 5×10^6 molecules cm^{-3} and HO rate coefficients from *Atkinson* [1994]. Variability was plotted as a function of lifetime rather than HO rate constants to be consistent with previous literature. An estimated rate constant for the m,p-xylene coeluted pair was made by simply averaging the respective rate constants [*Atkinson*, 1994]. The data were fit by a power law expression of the form

$$\sigma = Y_0 + A\,\tau^b, \quad (2)$$

which is a different expression than used previously to treat remote and rural data [*Jobson et al.*, 1998, 1999]. The inclusion of Y_0 is physically reasonable in this near source environment where mixing ratio variability would be strongly influenced by temporal variations in emission strengths, mixed layer heights, and wind speeds. Such influences at the point of emission may not be as apparent in more remote environments. Assuming a local lifetime will not influence the value of *b* but will influence the other parameters [*Jobson et al.*, 1999]. The variability values and HO rate constants are listed in Table 3 and the parameter values for equation (1) are listed in Table 4. Several species examined in section 5 are not plotted, notably the C_4 and C_5 alkenes which appeared to be good vehicle exhaust tracers.

Table 4. Values of Power Law Fitting Parameters to the Variability-Lifetime Trends

Parameter	HSC Source	Roadway Source
Y_o	0.61 ± 0.08	0.85 ± 0.05
A	0.41 ± 0.09	0.06 ± 0.04
b	−0.48 ± 0.08	−0.73 ± 0.19
Chi^2	0.97	6.50

The dynamic range of these species was not quantified; a large fraction of the ambient data were below the instrument detection limits. The standard deviations determined from such truncated frequency distributions are thus anomalously low. The data for 1-pentene from both the NOAA instruments are shown to illustrate this point. About 10% of the 1-pentene data from both instruments were below detection limits. The 1-pentene variability as measured by the NOAA-2 instrument falls well below the roadway source trend line.

[23] The differences in sampling frequency and sample integration times between the NOAA instruments could give rise to different statistical distributions for species measured in common. Longer sampling integration times and lower sampling frequency of the NOAA-2 instrument would tend to yield data that is less variable than the NOAA-1 instrument. This was indeed observed for the two species measured in common and whose dynamic range was quantified, i-pentane and hexane, though the differences were small. Given this potential systematic bias, trend lines through the data were restricted to data from a single instrument. The HSC source trend line was defined only by NOAA-1 data while the roadway source trend was defined by only NOAA-2 data.

[24] It is interesting that species measured by the NOAA-1 instrument and identified in section 5 as being impacted by industrial emissions defined a coherent power law trend (HSC source), while the vehicle exhaust tracers measured by the NOAA-2 instrument defined another trend (roadway source). The trends group species with similar source-sink distributions. Isobutane displayed a greater variability than the HSC source trend line, implying that it has a source that is not common to the HSC trend species. Isobutane was excluded form the HSC source fit as a distinct outlier. While i-pentane fit the roadway source trend very well, giving weight to its use as a tracer for this source type, n-pentane appeared to be an outlier. n-Pentane displayed a much greater variability than the roadway source trend line even though its abundance relative to i-pentane was consistent with vehicle exhaust. A potential reason for the larger variability is an underestimation of its mixing ratio at low levels. Species measured by the NOAA-2 instrument and noted as having industrial impacts in section 5 (methylcyclohexane, cyclohexane, isopropylbenzene, and hexane) in addition to 2,2,4-trimethylpentane all displayed greater variability than the roadway trend and appear to define a trend that parallels the HSC source line. This is evidence that the trend lines were defining different hydrocarbon source types and where not simply a result of sampling frequency differences between the NOAA instruments. The gasoline additive MTBE displayed a much greater variability than the roadway source trend line.

[25] The power law fits yielded a significant intercept (Y_o) indicating that an inert gas from these sources would still have a significantly broad lognormal mixing ratio distribution. This implies variability in emissions rates and dispersion rates, amounting to a mixing ratio spread of about 2 orders in magnitude. This information would be pertinent for evaluating dispersion and mixing in chemical transport models of the La Porte area. Carbon monoxide, a product of combustion and an often used tracer of anthropogenic sions, had a σ value of 0.50, much smaller than the trend line intercepts. The lower variability of CO is consistent with a significant atmospheric photochemical source from methane and other hydrocarbon oxidation, making its atmospheric distribution more homogeneous than that of species whose sources are only primary emissions. The lifetime dependence for the roadway source was -0.73 ± 0.19. The large uncertainty was driven by the relatively small lifetime range covered by data and a large Y_o, so that only species more reactive than toluene begin to display a variability significantly greater than Y_o. To better define the roadway source lifetime dependence, species more reactive than the trimethylbenzenes need to be measured. Given the uncertainty in the *b*, the roadway source and HSC source did not display a significantly different lifetime dependence. The main difference between the trends was a slightly lower intercept (Y_o) and a much larger pre-exponential factor (A) for the HSC trend. It is noted that an appearance of a coherent trend is only possible over a wide range of hydrocarbon reactivity, and that separating the data into source groups following the results in section 5 allowed coherent trends to be revealed in the La Porte data.

3.7. Hydrocarbon Reactivity

[26] Of the species noted with significant industrial source impacts, 1-butene, propene, and ethene will have the most impact on ozone production in Houston. Ozone production from the oxidation of these alkenes is very efficient [*Carter*, 1994], a result of their rapid reaction with HO and the generation of more reactive and photolabile aldehydes. A common measure to compare relative impacts of different hydrocarbons on urban ozone formation is to compare their HO loss frequencies, calculated from the product of the hydrocarbon concentration and its HO reaction rate coefficient. The loss frequency comparison is essentially comparing the initial rate of peroxy radical formation, the rate limiting step in ozone formation. The actual amount of ozone produced by a particular hydrocarbon is dependent on its oxidation mechanism and ambient conditions, including the abundance of other hydrocarbons and NO_x concentrations [*Carter*, 1994]. However, the hydrocarbon loss frequency analysis provides a simple means for comparing the impact on ozone production from different species.

[27] Figure 12 depicts the HO loss frequency due to reaction with different compound classes (alkenes, alkanes, aromatics) for the measurement period at La Porte as observed by the NOAA instruments for all species measured. Isoprene is not considered in the analysis as it is a locally emitted biogenic species but would contribute significantly as a local HO sink. Periods of exceptionally high loss frequencies were observed ($>50\ s^{-1}$) due to ethene and propene. For the species measured by the NOAA-2 instrument, periods of relative high loss frequencies ($>10\ s^{-1}$) were observed usually due to alkenes although the aromatics and alkanes were the dominant reactants on occasion. The figure illustrates the dominance of ethene and propene during periods of maximum hydrocarbon reactivity.

[28] To better understand conditions when ozone production occurs, the frequency distribution of daytime (0600 CST

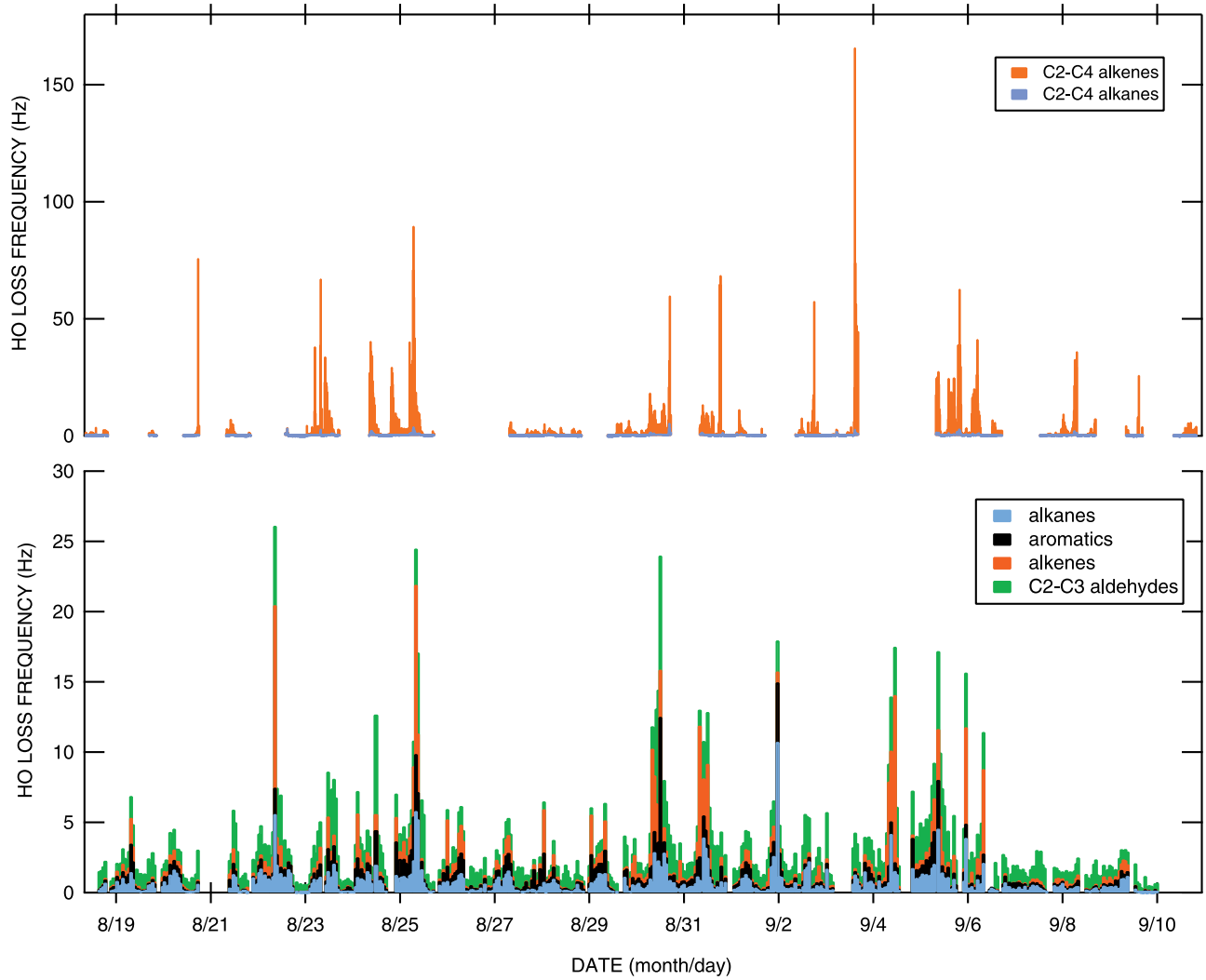

Figure 12. Time series of HO loss frequency due to reaction with hydrocarbons. Upper panel data from NOAA-1 instrument, lower panel data from NOAA-2 instrument.

to 1900 CST) HO loss frequencies for different species and compound classes were compared in Figure 13. The histograms for the aromatics and sum of alkanes >C_4 are not complete class groupings as many aromatics and alkanes were not measured. For example, the sum of the C_9 aromatics as measured by the PTR-MS were about twice as abundant as the sum of the trimethylbenzenes and isoprobylbenzene measured by the NOAA-2 instrument [*Kuster et al.*, 2004]. These data thus underestimate the actual HO loss frequency by about a factor of two. The alkane and aromatic class groupings and methanol have reasonably lognormal distributions with a similar range of loss frequencies, most of the data falling between 0.1 and 1 s^{-1}. The distributions of HCHO, C_2-C_3 aldehydes, and CO are likewise similar in magnitude, displaying less variability than other species, with a mode around 1 s^{-1} and a range between 0.2 and 10 s^{-1}. In contrast the light alkenes display a wide range of loss frequencies and some extreme values; 5% of the propene data had loss frequencies >10 s^{-1} compared to 3% for ethene. The influence of 1-butene is not terribly significant se of its lower mixing ratio, however the proportion of data with loss frequencies greater than 1 s^{-1} is similar to that of 1,3-butadiene, 6% and 9% respectively. Not shown are the sum of the other measured C_4, C_5 and C_6 alkenes which yielded loss frequency distributions similar to 1,3-butadiene, with a mode around 0.1 s^{-1} and 7% of the data with loss frequencies >1 s^{-1}. Thus the major impact on ozone photochemistry by petrochemical emissions lies in the often large loss frequencies for ethene and propene.

[29] Also shown is the loss frequency for a major radical chain termination reaction in urban photochemistry, that between HO and NO_2 to form HNO_3. This reaction displays a lognormal loss frequency distribution with a mode at 1.4 s^{-1}. This distribution is significantly wider than that of CO but seldom are chain termination frequencies greater than 10 s^{-1}. Figure 14 shows the daytime histogram of the NO_2 loss frequency (chain termination), summed hydrocarbon and CO loss frequencies (chain initiation), and the HO chain length given by the chain initiation to chain termination ratio. Plotted are data where the measurements of NO_2 and the various hydrocarbons where reasonably

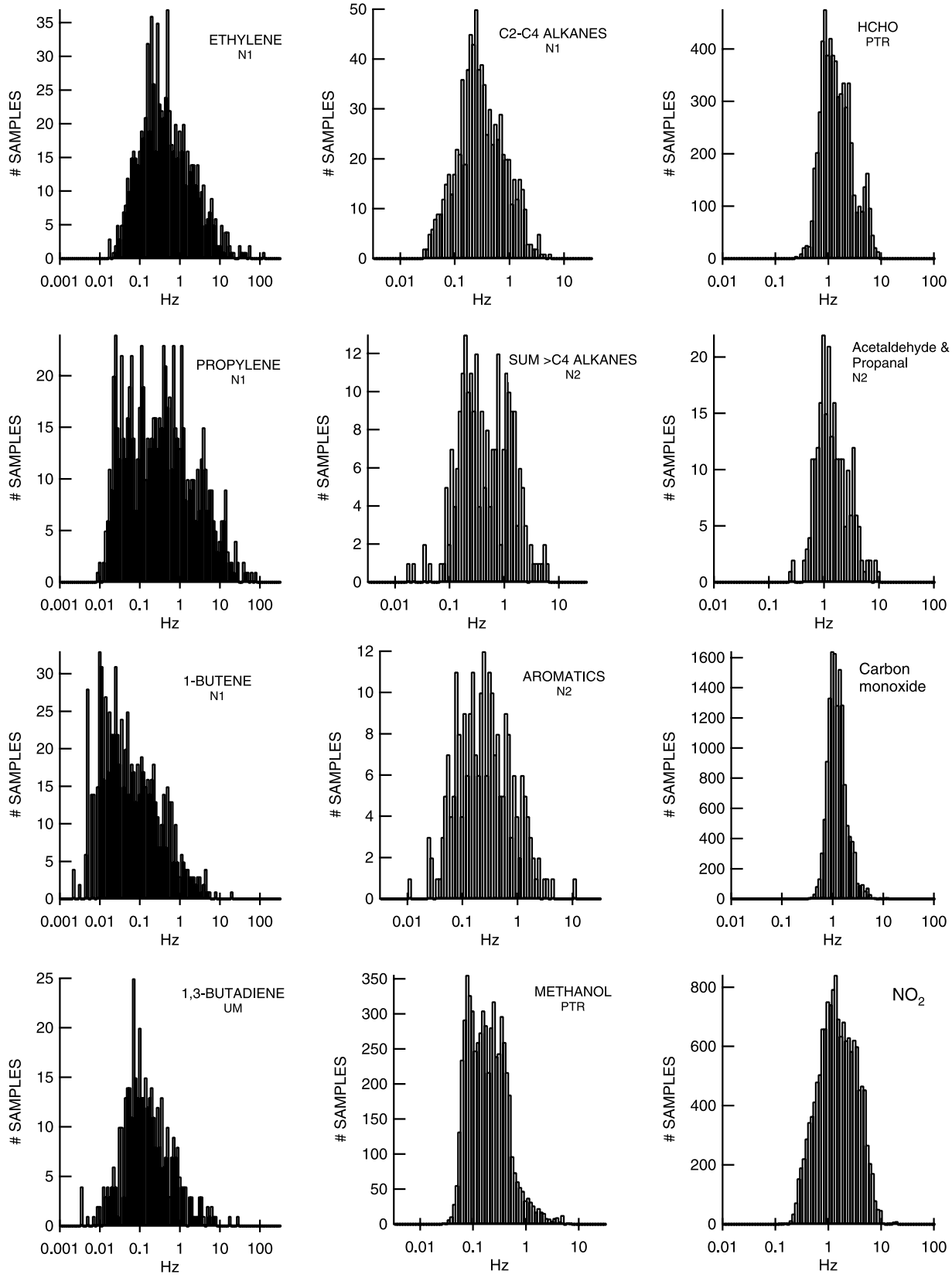

Figure 13. HO loss frequency histograms for selected hydrocarbons (N1, NOAA-1 data; N2, NOAA-2 data; UM, University of Miami data; PTR, proton transfer reaction mass spectrometer data) CO and NO_2.

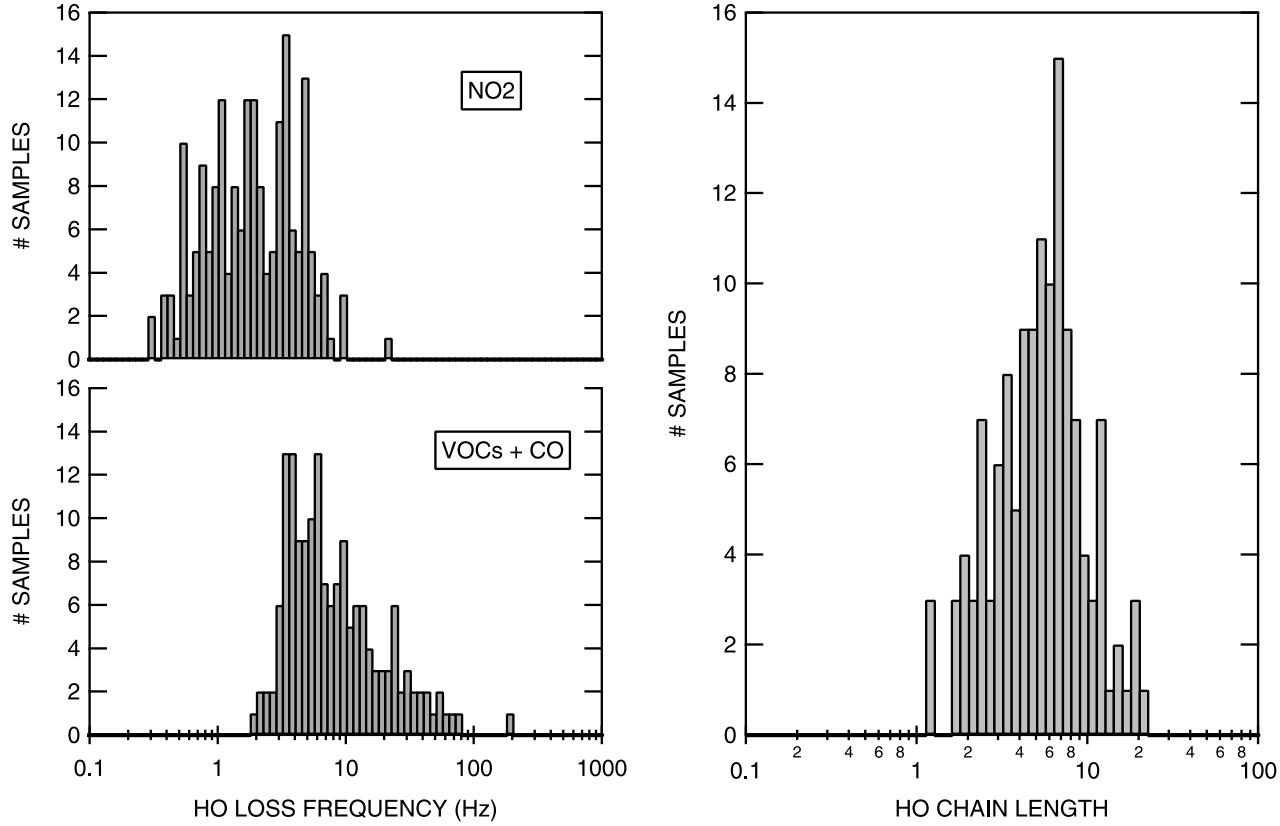

Figure 14. Panels to the left display histograms of daytime NO_2 and sum of hydrocarbon and CO loss frequencies. Panel to the right displays the histogram of daytime HO chain length given by the ratio of the coincident hydrocarbon and NO_2 loss frequencies shown.

coincident in time (±5 min) are thus are a subset of the data shown in Figure 13 with only 134 data points. The hydrocarbon and NO_2 loss frequencies were positively correlated though not strongly. The summed hydrocarbon and CO loss frequencies are quite skewed, but the resulting HO chain length is reasonably lognormal with a mode at 5.1 ± 0.2 (average 6.2 ± 3.9) and 13% of the data having chain lengths >10. The HO chain length is an important metric; the greater the chain length the more ozone that will be produced per NO_2 molecule oxidized [*Martinez et al.*, 2003], and this metric is easily related to chemical transport models to diagnose the oxidation capacity of the model. The chain length reported is that resulting from the dominant anthropogenic hydrocarbon chemistry and does not include the impact of locally emitted biogenic hydrocarbons such as isoprene.

3.8. La Porte Ozone Episodes

[30] Figure 15 displays the diel behavior of ozone, CO and NO_2 at La Porte. Highlighted in the figure are data from 30 and 31 August when ozone mixing ratios were at their highest. Ozone mixing ratios where greater than the 120 ppbv 1-hour National Ambient Air Quality Standard limit for more than 5 hours, with maximum ozone mixing ratios of 200 ppbv or more observed in the late afternoon around 1700 CST when local wind directions were from the south east sector. These da s were also characterized by overall high levels of CO and NO_2 in the afternoon. The late afternoon air masses appear to be arriving at the site on a sea breeze circulation. Of interest is whether the high ozone air masses where impacted by petrochemical emissions of olefins.

[31] To better understand the history of these high ozone air masses back trajectories were calculated from the vertical winds measured by a series of wind profilers deployed throughout the metropolitan area [*Berkowitz et al.*, 2004]. Light winds and the complication of land-sea breeze circulations often make the use of local wind direction as a vector leading back to a source meaningless in defining air mass origins. Thus it will be difficult to use local winds to understand the sources of industrial plumes observed at La Porte.

[32] Figure 16 displays hydrocarbon, CO, and ozone data for the 30 and 31 August ozone episodes. Shown are acetylene, ethene, propene, and i-pentane used as a source tracer for fossil fuel consumption. Trajectories were determined for each hour from 1300 to 1700 CST and these are illustrated in panels c and d in Figure 16. The 30 August trajectories show a pattern of slowing wind speeds and increasing stagnation in the afternoon, and a clockwise rotation or ''hooking'' pattern to the trajectories which brought emissions from the large refinery complex at the eastern end of the HSC (Baytown). The hydrocarbon data displayed a large increase in ethene and propene between

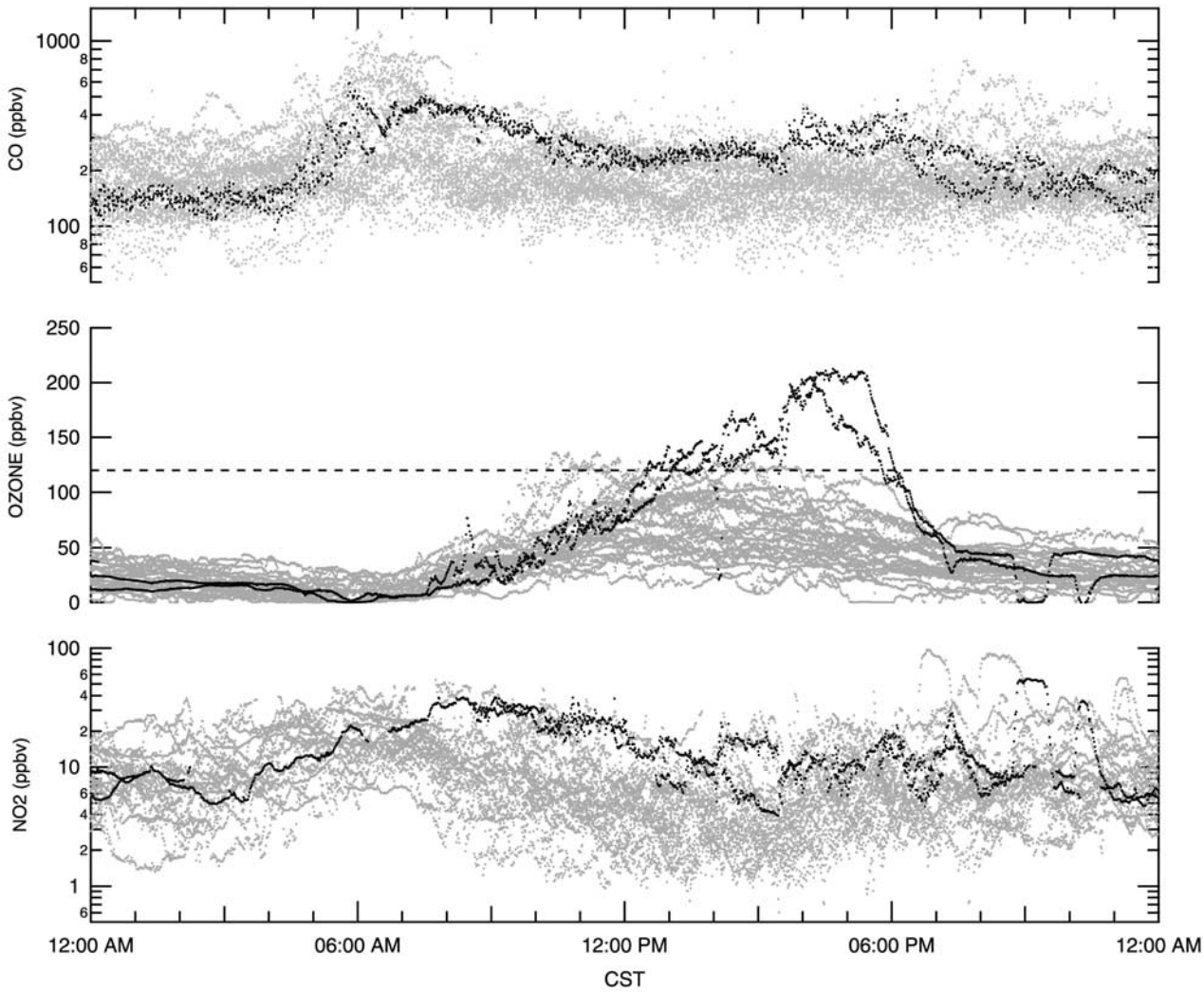

Figure 15. Diel cycles of CO, O_3, and NO_2 highlighting the ozone episode data from 30 and 31 August. Line through the ozone plot represents the 120 ppbv 1-hour NAAQS standard.

1415 and 1545 CST, with a corresponding increase in ozone of about 20 ppbv to an average mixing ratio of 162 ppbv during this period. The 1500 CST trajectory representative of this ethene plume passed over the Baytown refinery complex 2 hours previously. This complex appears to be a large emitter of ethene and aircraft studies have noted large ozone mixing ratios downwind of this facility. Interestingly acetylene also displayed a big increase at this time, with mixing ratios significantly higher in this plume than during the morning rush hour period. However i-pentane mixing ratios and as well as aromatic mixing ratios (benzene, toluene, C_2-benzenes) decreased, with CO mixing ratios remaining essentially unchanged. The increase in acetylene suggests that this complex may also be a source of acetylene. Emissions inventory for the HSC indicate acetylene emissions from the production of alkenes, from the manufacture of carbon black, and from the production of acetylene. The big increase in ozone at about 1600 CST was associated with trajectories that had passed near a refinery complex some 5–6 ho rlier and represent air masses than have been processed about twice as long as the 1500 air mass. Ozone mixing ratios in these air masses were on average 205 ppbv, and were accompanied by a 55 ppbv increase in CO. There is no evidence of an obvious impact of industrial alkene emissions in these more aged air masses although acetylene was again elevated. It is possible that the alkenes have been oxidized from these older plumes. Formaldehyde, as measured by the PTR-MS, displayed elevated mixing ratios (>20 ppbv) during the ozone episodes. Acetaldehyde and propanal mixing ratios were not significantly elevated during these periods, suggesting that ethene and not higher alkenes was the principal reactive hydrocarbon.

[33] The 31 August trajectories displayed a different behavior, with trajectories veering and hooking in a counterclockwise rather than clockwise fashion. These trajectories indicate that air masses arrived from the west side of the metropolitan area and only the 1300, 1400 and 1500 CST trajectories traveled over the HSC and city center. This time period is characterized by a plume in

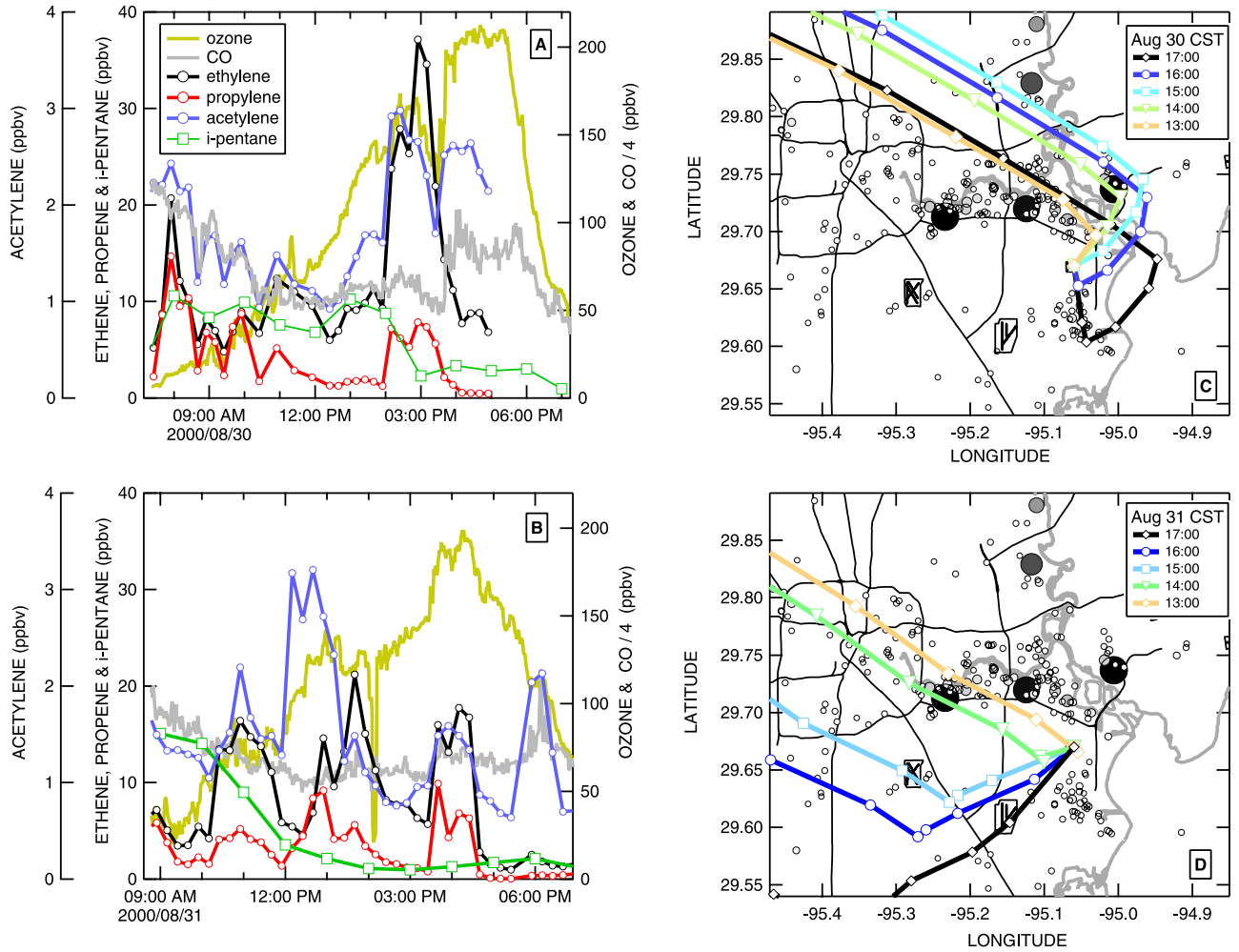

Figure 16. (a and b) time series of hydrocarbons (circles NOAA-1 data and squares NOAA-2 data), ozone, and CO during the 30 and 31 August ozone episodes observed at La Porte. (c and d) Corresponding back trajectories at hourly intervals in the afternoon.

acetylene (1200–1300) unassociated with elevated mixing ratios of other hydrocarbons or CO, and modestly elevated ethene and propene. The sharp increase in ozone mixing ratios (~40 ppbv) observed about 1530 and lasting till about 1645 was coincident with an increase in ethene (~10 ppbv) and propene (~6 ppbv) and again acetylene (~0.5 ppbv), with no obvious increase in other hydrocarbons. The 1600 CST trajectory did not pass over the HSC and encountered no known sources that might account for the ethene and propene plume. It is difficult to reconcile the trace gas behavior with these trajectories and may point to limitations in the trajectory calculations in defining air mass positions from the profiler network. These data indicate that acetylene may not be a good tracer of vehicle emissions since obvious strong sources exist in the HSC.

4. Conclusion

[34] Measurements of C_1-C_{10} hydrocarbons were made by 4 in-situ instruments at the La Porte super site from 18 August to 12 Septe during the Texas Air Quality 2000 field experiment. These data where analyzed to better understand the impact of petrochemical emissions of hydrocarbons on ambient concentrations and their potential impact on ozone formation in the Houston metropolitan area. The light alkanes and the light alkenes were determined to be the most impacted by petrochemical emissions. While frequency distributions of most hydrocarbons were lognormal, those of ethene, propene, and 1-butene were very skewed toward high values. The relative abundance of the C_2-C_4 alkanes was much greater than suggested by the vehicle exhaust profile determined from canisters samples collected in the Washburn Tunnel during the study. Natural gas and natural gas liquids used as petrochemical feed stocks could be important sources of light alkanes at La Porte. Variability-lifetime analysis showed coherent power law trends for two major source groups identified as roadway vehicle emissions and the Houston Ship Channel. This type of analysis could be usefully extended to the analysis of routine hydrocarbon data collected in the Houston metropolitan area to better understand the impact of HSC emissions throughout the area. Species identified as being severely impacted by

industrial emissions were ethane, ethene, propane, propene, n-butane, i-butane, 1-butene, hexane, cyclohexane, methylcyclohexane, isopropylbenzene, and styrene. It was observed that acetylene also appeared to be impacted by emissions sources in the HSC. Most aromatics and the longer chain alkanes displayed relative abundances that were consistent with roadway vehicle emissions as the dominant source. In general hydrocarbon reactivity was dominated by C_1-C_3 aldehydes, with ethene and propene occasionally dominating due to high concentration plumes and resulting HO loss frequencies >50 s^{-1}. From coincident measurements of NO_2, hydrocarbons and CO, the median daytime HO chain length was 5.1, with values greater than 10 observed 13% of the time. Back trajectory analysis of a severe ozone episode observed at La Porte on 30 August indicate that the air masses had been impacted by emissions from the HSC.

References

Atkinson, R. (1994), *Gas-Phase Tropospheric Chemistry of Organic Compounds*, *J. Chem. Phys. Ref. Data Monogr.*, vol. 2, edited by J. W. Gallagher, Am. Chem. Soc., Am. Inst. of Phys., Woodbury, N. Y.

Berkowitz, C. M., T. Jobson, G. Jiang, C. W. Spicer, and P. V. Doskey (2004), Chemical and meteorological characteristics associated with rapid increases of O_3 in Houston, Texas, *J. Geophys. Res.*, *109*, D10307, doi:10.1029/2003JD004141.

Borbon, A., H. Fontaine, M. Veillerot, N. Locoge, J. C. Galloo, and R. Guillermo (2001), An investigation into the traffic-related fraction of isoprene at an urban location, *Atmos. Environ.*, *35*, 3749–3760.

Carter, W. P. L. (1994), Development of ozone reactivity scales for volatile organic compounds, *J. Air Waste Manage. Assoc.*, *44*, 881–899.

Choi, Y.-J., and S. H. Ehrman (2004), Investigation of sources of volatile organic carbon in the Baltimore area using highly time-resolved measurements, *Atmos. Environ.*, *38*, 775–791.

Colman, J. J., D. R. Blake, and F. S. Rowland (1998), Atmospheric residence time of CH3Br estimated from the Junge spatial variability relation, *Science*, *281*, 392–396.

Conner, T. L., W. A. Lonneman, and R. L. Seila (1995), Transportation-related volatile hydrocarbon source profiles measured in Atlanta, *J. Air Waste Manage. Assoc.*, *45*, 383–394.

Daum, P. H., L. I. Kleinman, S. R. Springston, L. J. Nunnermacker, Y.-N. Lee, J. Weinstein-Lloyd, J. Zheng, and C. M. Berkowitz (2003), A comparative study of O_3 formation in the Houston urban and industrial plumes during the 2000 Texas Air Quality Study, *J. Geophys. Res.*, *108*(D23), 4715, doi:10.1029/2003JD003552.

Ehhalt, D. H., F. Rohrer, A. Wahner, M. J. Prather, and D. R. Blake (1998), On the use of hydrocarbons for the determination of tropospheric HO concentrations, *J. Geophys. Res.*, *103*, 18,981–18,997.

Environmental Protection Agency (EPA) (2000), National air pollutant emission trends 1900–1998, *Rep. EPA 454/R-00-002*, Off. of Air Qual. Plann. and Stand., Research Triangle Park, N. C.

Environmental Protection Agency (EPA) (2001) National air quality and emissions trends 1999, *Rep. EPA 454/R-01-004*, Off. of Air Qual. Plann. and Stand., Research Triangle Park, N. C.

Fraser, M. P., G. R. Cass, and B. R. T. Simoneit (1998), Gas-phase and particle-phase organic compounds emitted from motor vehicle traffic in a Los Angeles roadway tunnel, *Environ. Sci. Technol.*, *32*, 2051–2060.

Fujita, E. M. (2001), Hydrocarbon source apportionment for the 1996 Paso del Norte Ozone Study, *Sci. Total Environ.*, *276*, 171–184.

Geyer, A., et al. (2003), Direct observations of daytime NO_3: Implications for urban boundary layer chemistry, *J. Geophys. Res.*, *108*(D12), 4368, doi:10.1029/2002JD002967.

Haagen-Smit, A. J. (1952), Chemistry and physiology of Los Angeles Smog, *Ind. Eng. Chem.*, *44*, 1342–1346.

Hamrud, M. (1983), Residence time and spatial variability for gases in the atmosphere, *Tellus, Ser. B*, *35*, 295–303.

Harley, R. A., M. P. Hannigan, and G. R. Cass (1992), Respeciation of organic gas emissions and the detection of excess unburned gasoline in the atmosphere, *Environ. Sci. Technol.*, *26*, 2395–2408.

Jobson, B. T., D. D. Parrish, P. Goldan, W. Kuster, F. C. Fehsenfeld, D. R. Blake, N. J. Blake, and H. Niki (1998), Spatial and temporal variability of nonmethane hydrocarbon mixing ratios and their relation to photochemical lifetime, *J. Geophys. Res. 103*, 13,557–13,567.

Jobson, B. T., S. A. McKeen, D. D. Parrish, F. C. Fehsenfeld, D. R. Blake, A. H. Goldstein, S. M. Schauffler, and J. W. Elkins (1999), Trace gas mixing ratio variability versus lifetime in the troposphere and stratosphere: Observations, *J. Geophys. Res.*, *104*, 16,091–16,113.

Johnston, N. A. C., J. J. Colman, D. R. Blake, M. J. Prather, and F. S. Rowland (2002), On the variability of tropospheric gases: Sampling, loss patterns, and lifetime, *J. Geophys. Res.*, *107*(D11), 4111, doi:10.1029/2001JD000669.

Karl, T., P. J. Crutzen, M. Mandl, M. Staudinger, A. Guenther, A. Jordan, R. Fall, and W. Lindinger (2001), Variability-lifetime relationship of VOCs observed at the SonnBlick Observatory 1999—Estimation of HO densities, *Atmos. Environ.*, *35*, 5287–5300.

Karl, T., T. Jobson, W. C. Kuster, E. Williams, J. Stutz, R. Shetter, S. R. Hall, P. Goldan, F. Fehsenfeld, and W. Lindinger (2003), Use of proton-transfer-reaction mass spectrometry to characterize volatile organic compound sources at the La Porte super site during the Texas Air Quality Study 2000, *J. Geophys. Res.*, *108*(D16), 4508, doi:10.1029/2002JD003333.

Kirchstetter, T. W., B. C. Singer, R. A. Harley, G. R. Kendall, and W. Chan (1996), Impact of oxygenated gasoline use on California light duty vehicle emissions, *Environ. Sci. Technol.*, *30*, 661–670.

Kleinman, L. I., P. H. Daum, D. Imre, Y.-N. Lee, L. J. Nunnermacker, S. R. Springston, J. Weinstein-Lloyd, and J. Rudolph (2002), Ozone production rate and hydrocarbon reactivity in 5 urban areas: A cause of high ozone concentration in Houston, *Geophys. Res. Lett.*, *29*(10), 1467, doi:10.1029/2001GL014569.

Kuster, W. C., B. T. Jobson, T. Karl, D. Reimer, E. Apel, P. D. Goldan, and F. C. Fehsenfeld (2004), Intercomparison of volatile organic carbon measurement techniques and data at La Porte during the TexAQS2000 Air Quality Study, *Environ. Sci. Technol.*, *38*, 221–228.

Lenschow, D. H., and D. Gurarie (2002), A simple model for relating concentrations and fluctuations of trace reactive species to their lifetimes in the atmosphere, *J. Geophys. Res.*, *107*(D24), 4805, doi:10.1029/2002JD002526.

Lippmann, M. (1991), Health effects of tropospheric ozone, *Environ. Sci. Technol.*, *25*, 1954–1962.

Lonneman, W. A. (1998), *Comparison of Hydrocarbon Composition in Los Angeles for the years 1968 and 1997, Measurement of Toxic and Related Air Pollutants, Proceedings of a Specialty Conference*, vol. 1, Air and Waste Manage. Assoc., Cary, N. C.

Martinez, M., et al. (2003), OH and HO_2 concentrations, sources, and loss rates during the Southern Oxidants Study in Nashville, Tennessee, summer 1999, *J. Geophys. Res.*, *108*(D19), 4617, doi:10.1029/2003JD003551.

Mayrsohn, H., J. H. Crabtree, M. Kuramoto, R. D. Sothern, and S. H. Mano (1977), Source reconciliation of atmospheric hydrocarbons 1974, *Atmos. Environ.*, *11*, 189–192.

McGaughey, G. R., N. R. Desai, D. T. Allen, R. L. Seila, W. A. Lonneman, M. P. Fraser, R. A. Harley, A. K. Pollack, J. M. Ivy, and J. H. Price (2004), Analysis of motor vehicle emissions in a Houston tunnel during the Texas Air Quality Study 2000, *Atmos. Environ.*, *38*, 3363–3373.

McLaren, R., D. L. Singleton, J. Y. Lai, B. Khouw, E. Singer, Z. Wu, and H. Niki (1996), Analysis of motor vehicle sources and their contribution to ambient hydrocarbon distributions at urban sites in Toronto during the Southern Ontario Oxidants Study, *Atmos. Environ.*, *30*, 2219–2232.

Odum, J. R., T. P. W. Jungkamp, R. J. Griffin, R. C. Flagan, and J. H. Seinfeld (1997), The atmospheric aerosol forming potential of whole gasoline vapor, *Science*, *276*, 96–98.

Parrish, D. D., et al. (1998), Internal consistency tests for evaluation of measurements of anthropogenic hydrocarbons in the troposphere, *J. Geophys. Res.*, *103*, 22,339–22,359.

Roberts, J. M., et al. (2003), An examination of the chemistry of peroxycarboxylic nitric anhydrides and related volatile organic compounds during Texas Air Quality Study 2000 using ground-based measurements, *J. Geophys. Res.*, *108*(D16), 4495, doi:10.1029/2003JD003383.

Rogak, S. N., U. Pott, T. Dann, and D. Wang (1998), Gaseous emissions from vehicles in a traffic tunnel in Vancouver, *British Columbia, J. Air Waste Manage. Assoc.*, *48*, 604–615.

Rosen, R. S., E. C. Wood, P. J. Wooldridge, J. A. Thornton, D. A. Day, W. Kuster, E. J. Williams, B. T. Jobson, and R. C. Cohen (2004), Observations of total alkyl nitrates during Texas Air Quality Study 2000: Implications for O_3 and alkyl nitrate photochemistry, *J. Geophys. Res.*, *109*, D07303, doi:10.1029/2003JD004227.

Ryerson, T. B., et al. (2003), Effect of petrochemical industrial emissions of reactive alkenes and NO_x on tropospheric ozone formation in Houston, Texas, *J. Geophys. Res.*, *108*(D8), 4249, doi:10.1029/2002JD003070.

Sagebiel, J. C., B. Zielinska, W. R. Pierson, and A. W. Gertler (1996), Real-world emissions and calculated reactivities of organic species from motor vehicles, *Atmos. Environ.*, *30*, 2287–2296.

Schauer, J. J., M. P. Fraser, G. R. Cass, and B. R. T. Simoneit (2002), Source reconciliation of atmospheric gas phase and particle phase pollutants during a severe photochemical smog episode, *Environ. Sci. Technol.*, *36*, 3806–3814.

Solomon, P., E. Cowling, G. Hidy, and C. Furiness (2000), Comparison of scientific findings from major ozone fields studies in North America an Europe, *Atmos. Environ.*, *34*, 1885–1920.

Watson, J. G., J. C. Chow, and E. M. Fujita (2001), Review of volatile organic compound source apportionment by chemical mass balance, *Atmos. Environ.*, *35*, 1567–1584.

Williams, J., et al. (2000), Variability-lifetime relationship for organic trace gases: A novel aid to compound identification and estimation of HO concentrations, *J. Geophys. Res.*, *105*, 20,473–20,486.

Williams, J., V. Gros, B. Bonsang, and V. Kazan (2001), HO cycle in 1997 and 1998 over the southern Indian Ocean derived from CO, radon, and hydrocarbon measurements made at Amsterdam Island, *J. Geophys. Res.*, *106*, 12,719–12,725.

E. C. Apel and T. Karl, Atmospheric Chemistry Division, National Center for Atmospheric Research, 1850 Table Mesa Drive, Boulder, CO 80020, USA.

C. M. Berkowitz and B. T. Jobson, Pacific Northwest National Laboratory, Richland, WA 99352, USA. (tom.jobson@pnl.gov)

F. C. Fesenfeld, P. D. Goldan, W. C. Kuster, and E. J. Williams, NOAA Aeronomy Laboratory, R/E/AL7, 325 Broadway, Building 22, Boulder, CO 80303, USA.

W. A. Lonneman, National Exposure Research Laboratory, Senior Environmental Employment Program, U.S. Environmental Protection Agency, Research Triangle Park, NC 27711, USA.

D. Riemer, Rosenstiel School of Marine and Atmospheric Science, University of Miami, Miami, FL 33149, USA.